



An Introduction to the Vector Meson

F. Nichitiu*

INFN – Laboratori Nazionali di Frascati, P.O. Box 13, I 00044-Frascati (Roma) Italy

Abstract

In the present paper we survey the present status of the experimental knowledge on vector mesons built from light quarks.

1. ($q\bar{q}$) systems

Using the non relativistic quark model, most of the many hadronic states known nowadays can be described as states made of only q and \bar{q} . S.Godfrey and N.Isgur¹ have proposed a relativised quarkonium model which describes all the mesons from the pion to the heaviest epsilon using a unified framework.

Ignoring the heavy quarks, there are nine possible ($q\bar{q}$) combinations (quark flavour: u,d,s) which are grouped into an octet and a singlet. The mass formula for an octet is given by the Gell-Mann-Okubo formula:

$$m_{I=0}^2 = (4m_{I=1/2}^2 - m_{I=1}^2)/3. \quad (1)$$

The states with the same I, J and P (and additive quantum numbers) can mix due to SU(3) breaking, a mixing which in general is mass dependent. Because of this, it is common to group the mesons into nonets rather than octets and singlets.

If the quark flavour decomposition for a pure singlet and octet is

- - singlet: $I=0$ $(u\bar{u} + d\bar{d} + s\bar{s})/\sqrt{3}$
- - octet: $I=1$ $u\bar{d}; (u\bar{u} + d\bar{d})/\sqrt{2}; d\bar{u}$
- - $I=1/2$ $u\bar{s}; d\bar{s}$
- - $I=1/2$ $s\bar{d}; s\bar{u}$
- - $I=0$ $(u\bar{u} + d\bar{d} - 2s\bar{s})/\sqrt{6}$

PACS.: 11.80.Et; 11.80.Gw; 13.75.Cs; 14.40.Cs

Invited talk at the "NATO Summer School on Meson Spectroscopy and Confinement Problems", London, GB, 6–13 June 1995

* On leave of absence from IFA-Bucharest, Romania

then the two $I=0$ physical states of a given nonet

$$|Phys - a\rangle = |8\rangle \cos(\theta) - |1\rangle \sin(\theta) \quad (2)$$

$$|Phys - b\rangle = |8\rangle \sin(\theta) + |1\rangle \cos(\theta) \quad (3)$$

can have such a mixing angle that one of the physical states can be pure or mostly $|s\bar{s}\rangle$. This angle is named 'ideal' and is given by $\tan \theta = 1/\sqrt{2}$ or $\theta = 35.3^\circ$.

The lowest vector nonet, $\rho(770)$, $K^*(892)$, $\omega(782)$ and $\phi(1020)$ is indeed ideally mixed; $\phi(1020)$ is practically a pure state of $|s\bar{s}\rangle$ and ω a pure state containing no strange quarks $|(u\bar{u} - d\bar{d})/\sqrt{2}\rangle$. It is believed that all the vector mesons are almost ideally mixed. This is an important fact which is used in phenomenological analysis of new vector meson states.

Assuming the mesons to be $q\bar{q}$ states, a pair of two $1/2$ spin 'particles' (fermions) with fractional charges (u and d forming an isodoublet), the quantum numbers permitted for a meson-nonet are grouped as :

- the normal (or natural) spin-parity series where $P=(-1)^J$ and $CP=+1$
 $0^{+-}; 1^{--}; 2^{++}; 3^{--}$, or using spectroscopic notation
 $^3P_0; ^3S_1; ^3P_2$,
- the unnatural spin-parity series where $P=(-1)^{J+1}$
 $0^{-+}; 1^{++}; 2^{-+}; 3^{++}$,
 $1^{+-}; 2^{--}; 3^{+-}$, or
 $^1S_0; ^3P_1; ^1D_2$,
 $^1P_1; ^3D_2$.

The $(q\bar{q})$ ground states are ($L=0$):

- $J^{PC} = 0^{-+}; ^1S_0$ pseudoscalar mesons, and
- $J^{PC} = 1^{--}; ^3S_1$ vector mesons.

The first radial excitation of the vector meson nonet is denoted by 2^3S_1 and the first orbital excitation by 1^3D_1 .

Some combinations of J, P and C are forbidden for normal $q\bar{q}$ states. The forbidden 'normal' $q\bar{q}$ states are all the mesonic states which belong to the normal spin-parity series ($P=(-1)^J$) for which $C = -P$, as well as the 0^{--} state. Such a quantum-mechanical selection rule for exotic J^{PC} assignments can exist only for mesons. These states are $0^{--}; 0^{+-}; 1^{-+}; 2^{+-}$ etc.

The present understanding of the strong interaction is that it is described by Quantum Chromo-Dynamics (QCD). This theory describes not only how quarks and antiquarks interact, but also predicts that the gluons which are the quanta of the field will themselves interact to form mesons. So, if a hadronic object (a meson) is composed only from valence gluons it is called a glueball (gluonia). The simplest colour-singlet gluonia are 2-gluon states with quantum numbers $0^{++}; 0^{-+}; 1^{-+}; 2^{-+}$... (the third is exotic, having non- $(q\bar{q})$ quantum numbers).

A gluonic vector state 1^{--} requires three gluons, which may exist as bound states just as baryons are made of 3 quarks. Exotic vector meson states which are not simple $q\bar{q}$ bound states can also exist if the state is composed of a mixture of valence quarks, antiquarks and gluons ($q\bar{q}g$) (hybrids) or contain many quark states ($qq\bar{q}\bar{q}$) denoted as $(q^2\bar{q}^2)$. These are multi-quark states which should not be confused with simple resonant

states of two mesons or with so-called molecular states. An unambiguous confirmation of such exotic states would be an important test of QCD and will give fundamental information on the behaviour of this theory in the confinement region.

2. Production of meson resonances; $e^+ e^-$ and γp .

An important part of the information on meson spectroscopy has been obtained from peripheral di-meson production where the dominant contribution comes from one pion exchange.

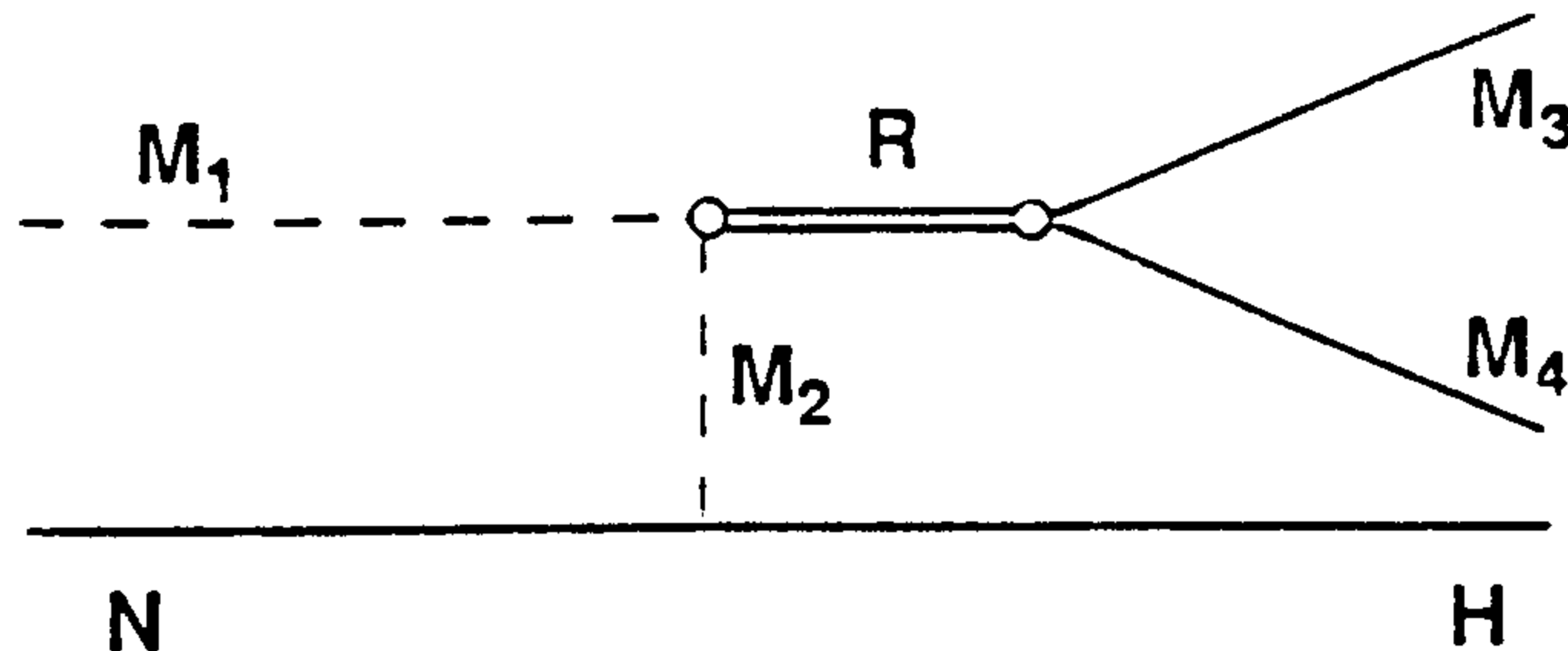


Figure 1: One Meson Exchange diagram. M_i are π or K mesons, N is the target nucleon and H is a nucleon or a hyperon.

Apart from the One-Meson-Exchange mechanism, Fig.1, basic for reactions of the type

- $\pi\pi \rightarrow \pi\pi$ or $(\bar{K}K)$
- $K\bar{K} (\pi) \rightarrow K\bar{K} (\pi)$,

there are also other mechanisms which contribute to the production of a multi-meson system in reactions such as:

- - diffractive reactions (meso/photo production)
- - $e^+ e^-$ collisions
- - $\gamma \gamma$ collision
- - central production,
- - nucleon antinucleon annihilation.

The first two, photoproduction and $e^+ e^-$ annihilation, Fig. 2, are very important for vector meson spectroscopy. Because the vector mesons have the same quantum numbers as the photon, 1^{--} ($I=0,1$), they will be easily produced either in $e^+ e^-$ collisions or in photoproduction. A very useful description of both types of vector meson production mechanisms is given by the so called Vector Dominance Model (VDM)²

The VDM arose much earlier than the quark model,³ but seems to be still compatible with it. The idea of the VDM, Fig. 3, consists in assuming that the interaction of a photon with hadrons is dominantly due to conversion of the γ into a hadronic vector meson ($J^{PC}=1^{--}$), which then interacts strongly with the hadronic target, as in any other strong collision. The Restricted VDM corresponds to the use of the low-lying vector meson states⁴ (ρ, ω, ϕ); the so called Extended (or Generalized) VDM⁵ uses a complete series of excited vector meson states ($\rho, \rho', \omega, \omega'$, etc). The latter is expected

to provide a good description of the electromagnetic interactions for a very large range of q^2 .

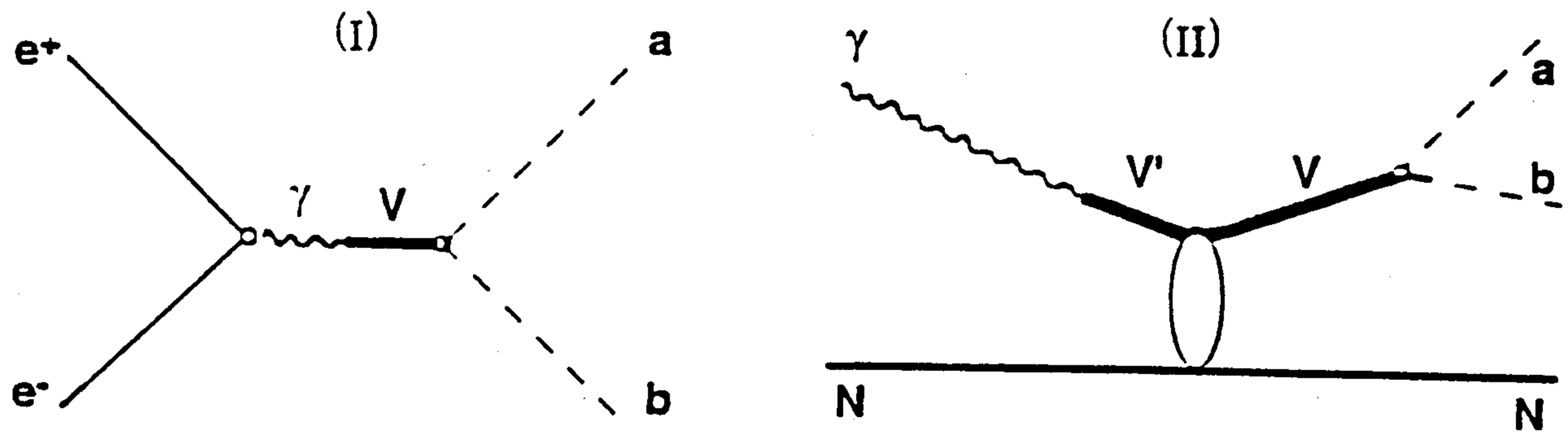


Figure 2: Vector meson production in e^+e^- (I) and γN (II).

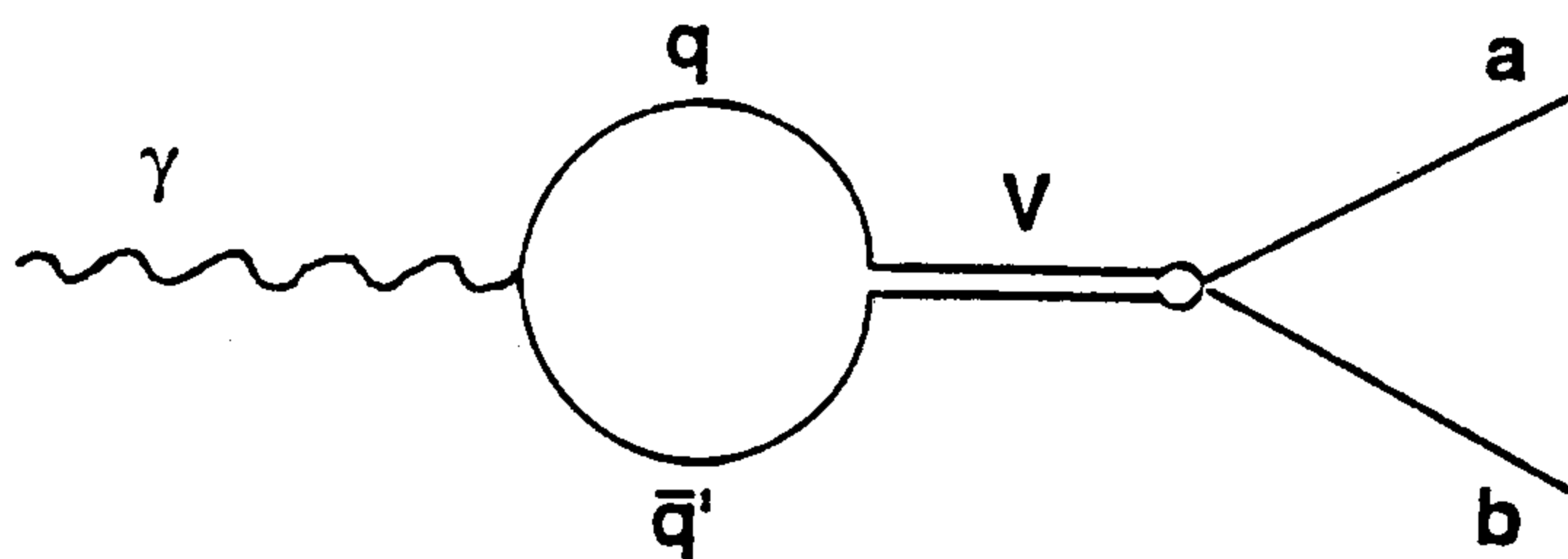


Figure 3: VDM view in quark language.

To explain the VDM in quark language, we restrict ourselves to the low energy domain, where q^2 is of the order of hadronic masses. Because the typical distance of interaction is of the same order of magnitude as the confinement radius ($R_c \sim 1/m_v \approx d \sim 1/\sqrt{q^2}$), the $q\bar{q}$ pair converted from the photon cannot be free (confinement effects will drive the $q\bar{q}$ pair to the nearby bound state with the same quantum numbers as the photon 1^{--} , therefore to vector mesons) and then the subsequent strong process takes place.

2.1. e^+e^- collisions.

When the e^+e^- center of mass energy is varied, one observes a series of peaks in the total cross section for some specific channels $e^+e^- \rightarrow$ hadrons. These peaks are due to the formation in the s channel of vector meson resonances which we interpret as quark-antiquark bound states. The general features of e^+e^- annihilation are given simply by a cross section expression calculated as a product of the usual $1/s$ dependence of the lepton pair production¹⁴ and a Breit-Wigner resonance shape for the vector meson:

$$\sigma(e^+e^- \rightarrow V) = \frac{3\pi}{s} \frac{\Gamma_{ee}\Gamma_V}{(m_V - \sqrt{s})^2 + \Gamma^2/4}. \quad (4)$$

The maximum of the cross section (σ at the peak) gives information on the leptonic width :

$$\Gamma_{ee} = \frac{m_V^2}{12\pi} \Gamma_V \sigma_{\text{peak}}, \quad (5)$$

where Γ_V is the total (hadronic) width of the vector meson. The connection between Γ_{ee} and the coupling constant is calculated by the explicit evaluation of the corresponding diagram and is given by :

$$\Gamma_{ee} = \frac{\alpha^2}{12} \left(\frac{4\pi}{g_V^2} \right) m_V; \quad (6)$$

the cross section will be given by :

$$\sigma = \frac{\pi^2}{m} \frac{(\alpha/g_V^2)}{(m_V - \sqrt{m})^2 + \Gamma^2/4}. \quad (7)$$

This semi-phenomenological picture appears to be very successful. In the framework of a potential model (an effective potential $V(r)$ between q and \bar{q}), the coupling constant between photon and vector meson will be proportional to the charge of the quark and to the value of the radial bound state wave function at the origin (at $r=0$).

In this way a very important relation is obtained between the leptonic width of a 1^{--} meson (Γ_{ee}) and the wave function of a $1^{--} q\bar{q}$ system which is connected with the corresponding quark structure of the vector meson:

$$\Gamma_{ee} = \frac{16\pi\alpha^2}{m_V^2} Q^2 |\Psi_{q\bar{q}}, (0)|^2. \quad (8)$$

Quantitative predictions for the coupling constant between vector meson and photon depend on the choice of the potential $V(r)$ which determines $\Psi(0)$. But there are some qualitative features which have some generality and have become important in data analysis.

In the non-relativistic limit, $\Psi(0)$ is non-zero only for S states and therefore only the 3S_1 and 2^3S_1 states (S radial excitation) should be coupled to e^+e^- . The orbital excitation 3D_1 and radial-orbital excitation 2^3D_1 will not be coupled to e^+e^- . These orbital excitations will be coupled only through relativistic corrections which involve the derivative of the wave function at the origin, or through configurations which mix with S states.

Also, because the radially excited states generally have more extended wave functions than those of the fundamental states (with $n=1$), the wave function at the origin, and therefore the coupling constant, are weaker, giving a smaller electronic width:

$$\Gamma_{ee}(L=0) > \Gamma_{ee}(L \neq 0) \quad (9)$$

$$\Gamma_{ee}(n > 1) < \Gamma_{ee}(n = 1). \quad (10)$$

A more extended wave function can be expected for multiquark states and therefore :

$$\Gamma_{ee}(\text{multiquark}) \ll \Gamma_{ee}(q\bar{q}). \quad (11)$$

Finally, if the $q\bar{q}$ potential is flavour independent and if we consider m_V roughly equal for all the vector mesons, an interesting rule appears :

$$\Gamma_{ee}(\rho, \omega, \phi)/Q^2 \simeq \text{constant}. \quad (12)$$

Here Q is the effective charge of the quarks involved. Because :

$$|\Psi(0)|^2/m_V^2 \simeq \text{constant}, \quad (13)$$

we can expect :

$$\Gamma_{ee} \sim Q^2. \quad (14)$$

For the fundamental vector meson nonet we have:

$$\Gamma_{ee}(\rho) = \left(\frac{1}{\sqrt{2}} \left(\frac{2}{3} + \frac{1}{3} \right) \right)^2 \frac{1}{\sqrt{2}} (u\bar{u} - d\bar{d}) \quad (15)$$

$$\Gamma_{ee}(\omega) = \left(\frac{1}{\sqrt{2}} \left(\frac{2}{3} - \frac{1}{3} \right) \right)^2 \frac{1}{\sqrt{2}}(u\bar{u} + d\bar{d}) \quad (16)$$

$$\Gamma_{ee}(\phi) = \left(-\frac{1}{3} \right)^2 (s\bar{s}) \quad (17)$$

which numerically means :

$$\begin{aligned} \Gamma_{ee}(\rho) : \Gamma_{ee}(\omega) : \Gamma_{ee}(\phi) &= 9 : 1 : 2 \\ \text{experimental} &= (8.8 \pm 2.6) : 1 : (1.7 \pm 0.4) \end{aligned} \quad (18)$$

A question is whether these ratios are correct for other vector meson nonets? The electromagnetic widths for the fundamental vector nonet taken from ⁷ are given below:

1^{--}	$\Gamma_{ee}(\text{keV})$	Γ_{ee}/Q^2	$g^2/4\pi$
$\rho(0.7699)$	6.77 ± 0.32	13.5	0.6
$\omega(0.7819)$	0.60 ± 0.02	10.8	8.
$\phi(1.0194)$	1.37 ± 0.05	12.3	4.

2.2. Photoproduction.

The VDM suggests that the vector meson 'produced' (created) from the photon is scattered on the target, becomes real and decays in the hadronic final state. If the initial state and the final one of this vector meson-target scattering are identical, this part of the interaction can be considered as elastic vector-meson-nucleon scattering and has the properties of a diffractive process:

- - the cross section is nearly energy independent,
- - there is a helicity transfer in the s channel from γ to the vector meson obeying so-called s-channel helicity conservation (SCHC), which is very important in practical analysis of experimental data (Partial Wave Analysis),
- - there is an exponential behaviour of the differential cross section

$$\frac{d\sigma}{dt} \sim e^{-b|t|} \quad (19)$$

with slope $b^2 \sim R$, where R is the radius of γN interaction.

The differential cross section for photoproduction processes is determined by the product of the coupling constant ($\gamma \rightarrow V$) and the corresponding hadronic cross section of the subprocess $VN \rightarrow VN$:

$$\frac{d\sigma}{dt}(\gamma N \rightarrow VN) = \alpha \frac{\pi}{g_V^2} \frac{d\sigma}{dt}(VN \rightarrow VN). \quad (20)$$

Assuming that the $VN \rightarrow VN$ scattering amplitude is purely imaginary (we are at high energies) and using the optical theorem which connects the total cross section to the imaginary part of the forward amplitude, we obtain:

$$\left. \frac{d\sigma}{dt}(\gamma N \rightarrow VN) \right|_{t=0} = \frac{\alpha}{16b} \frac{1}{g_V^2} \sigma_{\text{tot}}^2(VN), \quad (21)$$

from which is obtained an estimate of the photoproduction cross section:

$$\sigma(\gamma N \rightarrow VN) = \frac{\alpha}{16b} \frac{1}{g_V^2} \sigma_{\text{tot}}^2(VN). \quad (22)$$

The total cross section (VN) ought to be measured in an ideal experiment with V beams, but is in fact estimated by the vector quark content as for example by:

$$\sigma_{\text{tot}}(\Phi N) = (\sigma_{\text{tot}}^2(K^+ N) + \sigma_{\text{tot}}^2(K^- N) - \sigma_{\text{tot}}^2(\Pi^- N))^{1/2} \quad (23)$$

$$\sigma_{\text{tot}}(\rho N) = \frac{1}{2} (\sigma_{\text{tot}}(\pi^+ p) + \sigma_{\text{tot}}(\pi^- p)). \quad (24)$$

Due to the proportionality to the γV coupling constant in both expressions for vector meson production, in $e^+ e^-$ annihilation as well as in γp photoproduction the cross sections are related:

$$\sigma(e^+ e^- \rightarrow V \rightarrow \text{hadrons}) = \frac{32\pi^3 \alpha b}{m_V \sigma_{\text{tot}}^2(VN)} \sigma(\gamma N \rightarrow VN \rightarrow \text{hadrons}). \quad (25)$$

This formula allows therefore (in the framework of VDM) a comparison, i.e. a check on the theory; it can also be used to constrain a fit of the experimental data in order to find new states.

Some complications arise due to the fact that the 'two-step process' (vector meson scattering) is not only of the elastic type. There are so called 'off diagonal contributions' which are especially relevant for radial excitations (when the V' meson is different from the V meson as in fig.2).

In the 'intermediate energy' region, $e^+ e^-$ annihilation can be as complicated as any other interaction process in which the final hadronic state consists of a superposition of many resonances. It seems however that, in many cases, multiparticle production can be well described by a cascade of decays (as for example in the isobar model used in $p\bar{p}$ annihilation ¹²) of the type:

$$e^+ e^- \rightarrow \gamma \rightarrow (V) \rightarrow \begin{array}{l} X_1 \quad + \quad X_2 \\ \downarrow \quad \quad \downarrow \\ A + B \quad \downarrow \quad C + D \\ \quad \quad \quad \downarrow \\ \quad \quad \quad a + b \quad \text{etc.} \end{array} \quad (26)$$

Simple examples are :

$$e^+ e^- \rightarrow (\phi) \rightarrow \begin{array}{l} \rho \quad \pi \\ \downarrow \quad \downarrow \\ \pi \pi \end{array} \quad (27)$$

$$e^+ e^- \rightarrow (\rho') \rightarrow \begin{array}{l} \rho \quad (\pi\pi)_s \\ \downarrow \quad \downarrow \\ \pi \pi \end{array} \quad (28)$$

$$e^+ e^- \rightarrow (\phi') \rightarrow \begin{array}{l} K^* \quad + \bar{K} \\ \downarrow \quad \downarrow \\ K \pi \end{array} \quad (29)$$

The present experimental situation in the vector meson sector can be illustrated by the 'official' view of the PDG94 ⁷ and is given below :

		$I = 1$	$I = 0$		$I = 1/2$
$1^3 S_1$	1^{--}	$\rho(770)$	$\omega(782)$	$\phi(1024)$	$K^+(892)$
$2^3 S_1$	1^{--}	$\rho'(1450)$	$\omega'(1420)$	$\phi'(1680)$	$K'^+(1410)$
$3^3 D_1$	1^{--}	$\rho''(1700)$	$\omega''(1600)$?	$K''+(1680)$
$3^3 D_2$	2^{--}	?	?	?	$K_2(1820)$
$3^3 D_3$	3^{--}	$\rho_3(1690)$	$\omega_3(1670)$	$\phi_3(1850)$	$K_3(1780)$

3. ρ family

From the experimental point of view, the most important member of the vector meson nonet is the state with $I=1$, the ' ρ family'. Besides $\rho(770)$, up to some years ago only a second ρ with mass around 1600 MeV and width 400-500 MeV ($\rho'(1600)$) was known. Now it seems to be resolved into at least two ρ - states. The early evidence for this single second ρ came from some phase-shift analyses of the $\pi\pi$ system (to which the excited ρ state or states seems to be weakly coupled),¹³ as well as from the direct observation of enhancements in 4 pion spectra produced in e^+e^- collisions and in both electro and photo- production (for a list of experimental evidence of $\rho'(1600)$ see the mini-review of the PDG 84, ref⁸).

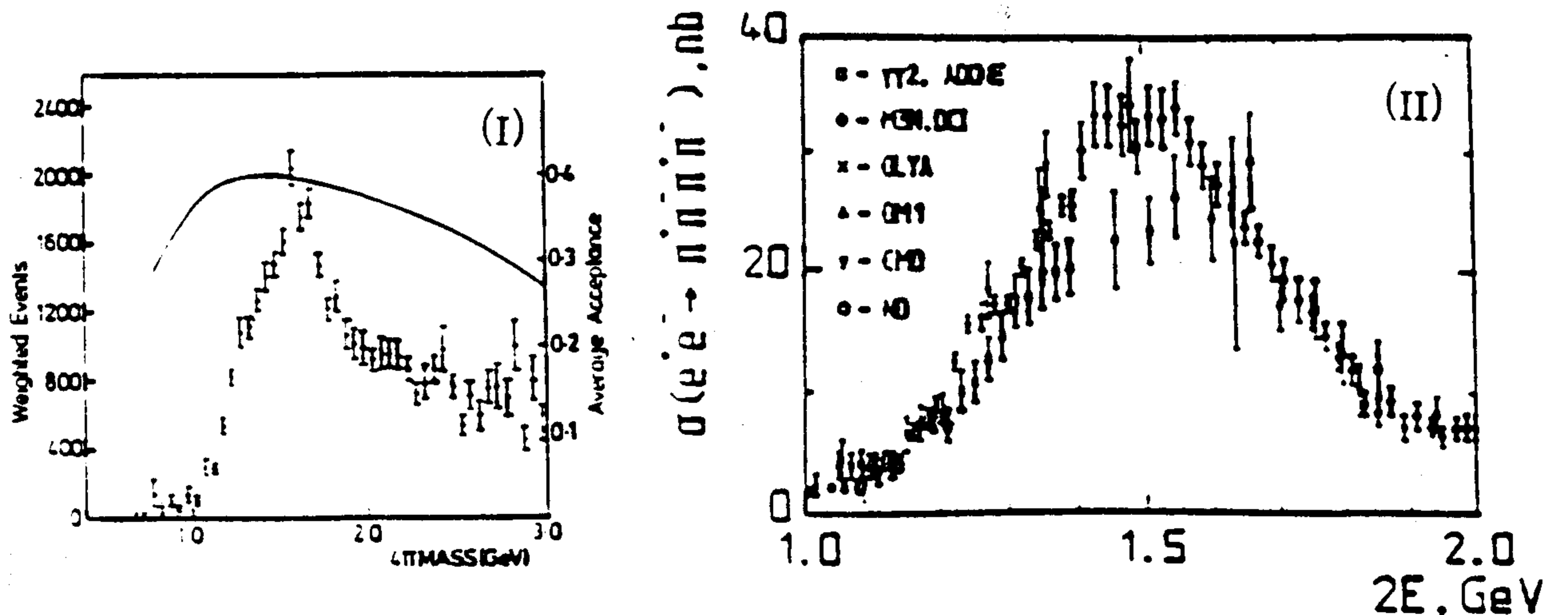


Figure 4: $2\pi^+2\pi^-$ from γp (I) and e^+e^- (II).

The first demonstration that data on e^+e^- annihilation into 2π and 4π can be understood in terms of the standard ρ and another two ρ excited states, ρ' and ρ'' , appeared in 1986 in ref. ⁶ and was adopted by the PDG in 1988 ⁷. The considerable uncertainty concerning the $\rho'(1600)$ 'bump' emerges from the complicated experimental situation, Figs.4 and 5. In reactions such as :

$$\gamma p \longrightarrow 2\pi^-2\pi^+p \quad (30)$$

$$e^+e^- \longrightarrow 2\pi^-2\pi^+ \quad (31)$$

a broad resonance peak is observed with mass and width in reasonably agreement in both reactions $m=1.57$ GeV $\Gamma=0.51$ GeV, but in the γp reaction over a significant non-resonant background. Fig.4 shows the experimental mass distribution for $2\pi^-2\pi^+$ from γp reactions ((I) ¹⁵) and e^+e^- annihilations (II, data quoted in ref. ^{11,36}).

For the $\pi^+\pi^-2\pi^0$ final state there is a very broad peak in the e^+e^- reaction and in γp there are two clear peaks at 1.25 GeV and at 1.60 GeV. The lower part of this spectrum is completely dominated by the $\omega\pi^0$ channel through γ photoproduction of $b_1(1250)$ (a non vector meson : $1^+(1^{+-})$ state). Fig.5 shows the experimental mass spectrum for $\pi^+\pi^-2\pi^0$ in γp reactions (I ¹⁶) before (a) and after (b) an ω cut ; and in e^+e^- annihilations (II, data quoted in ref. ^{11,36}).

The mass and width observed in mass distributions and in the energy dependence of the cross sections need not be the true resonance parameters because :

- - there may be a significant background which can interfere with the resonance,
- - in a multimeson final state there can exist more than one isobar (a quasi two-body state from the isobar decomposition of the multimeson final state) which can contribute, each with its own J^P .

A complete understanding of the final state can be therefore achieved only by a spin-parity analysis where a separation of different J^P contributions is obtained. The J^P determination is usually done using the premises of the 'SCHC' production mechanism in a complex fit of experimental angular distributions for different energy (mass) intervals.

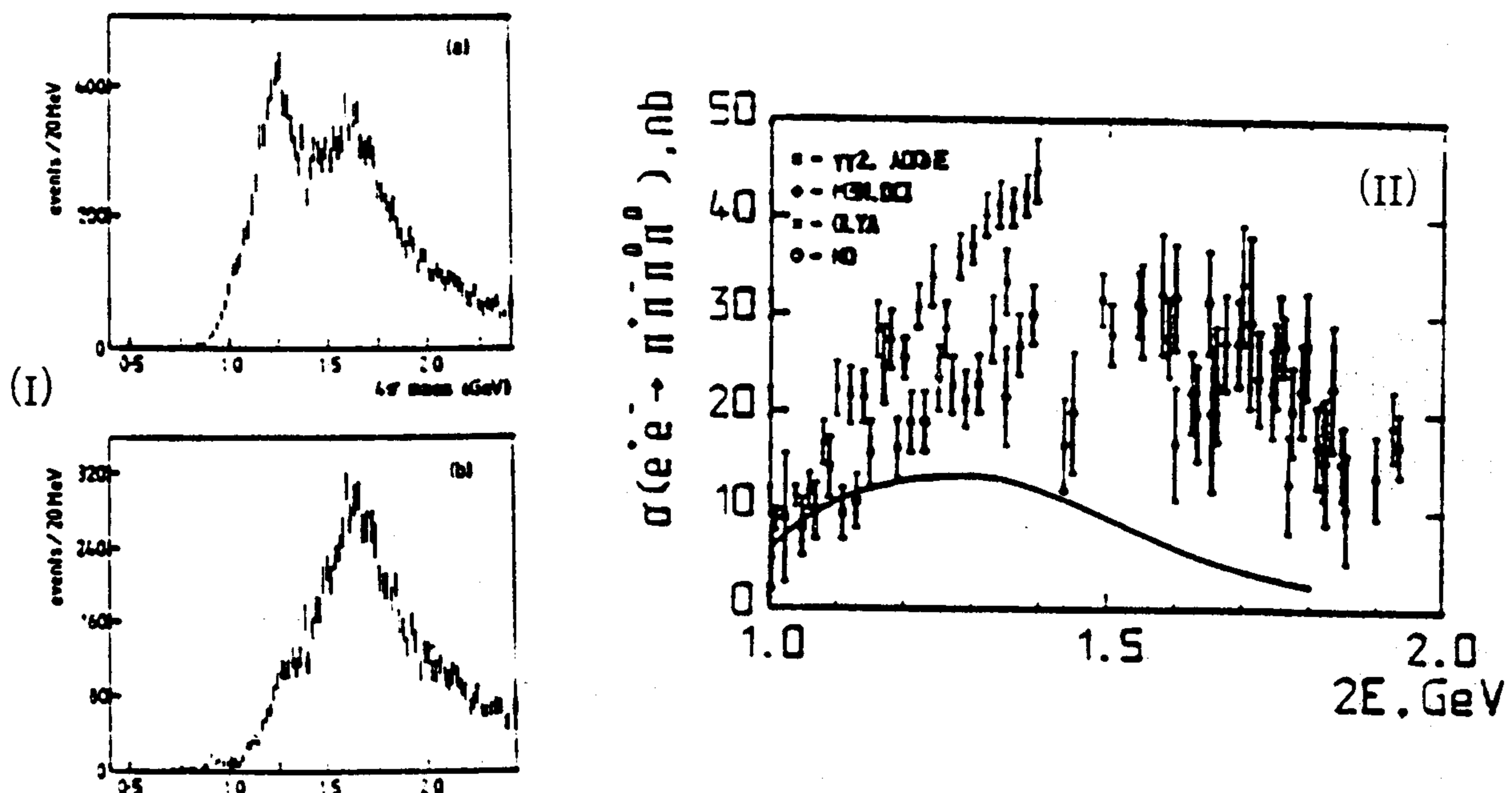


Figure 5: $\pi^+\pi^-2\pi^0$ from γp (I) and e^+e^- (II). In (I), (a) before and (b) after an ω cut.

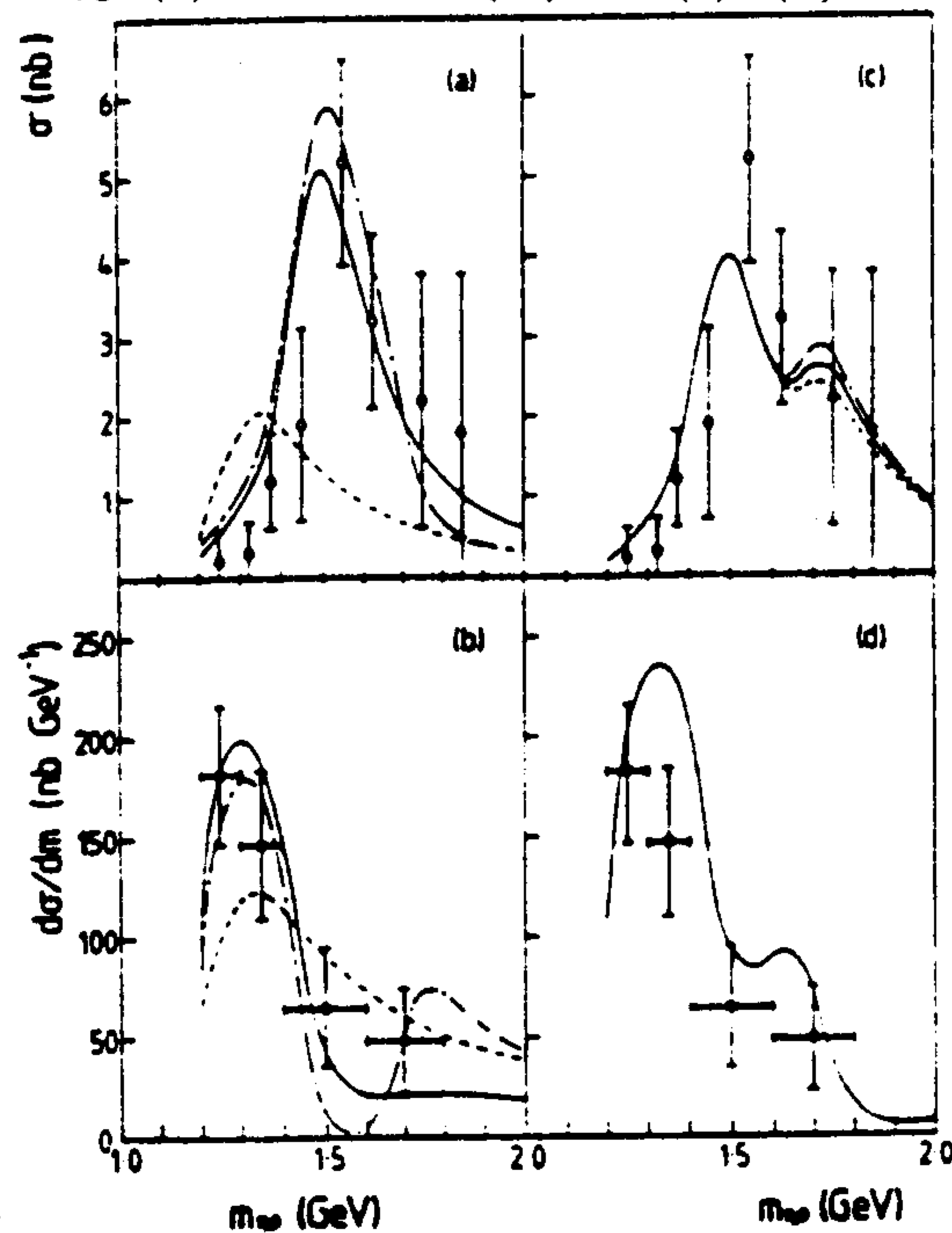


Figure 6: Fit of $e^+e^- \rightarrow \eta\rho$ (a) and (c), and $\gamma p \rightarrow \eta\rho$ (b) and (d)

The next step of the analysis will be the study of the mass dependence of each partial wave contribution (intensity of the PWA or partial wave cross section, and if it exists, the phase motion of the PW amplitude). An example of such a study is the analysis of $\eta\rho$ produced in diffractive γp reactions and in e^+e^- annihilations, Fig.6, done by Donnachie and Clegg¹⁰.

The mass spectra of $\eta\rho$ states with $J^P=1^-$ from diffractive photo-production and from e^+e^- annihilation appear at first sight to be completely incompatible. The apparent discrepancy was resolved through interferences between the tail of the $\rho(770)$

meson and two ρ' meson states.

This analysis points strongly to the existence of a ρ' resonance with a mass of about 1.47 GeV and a branching ratio into $\eta\rho$ of 3-4 % whose amplitude interferes with the tail of the ρ . The relative sign of the ρ' amplitude relative to that of $\rho(770)$ is different in e^+e^- annihilation and photoproduction. The contribution from a higher vector meson in the $\eta\rho$ channel seems to be only marginal.

In order to understand the structure of the equations used to fit the experimental data on the $\eta\rho$ final state produced in two different reactions (γp and e^+e^-) we recall here the specific Breit-Wigner forms of the partial wave amplitudes used in such cases. The Breit-Wigner partial wave amplitude for a simple transition shown in Fig.7 is given by:

$$T \sim \frac{\text{Vertex1} \cdot \text{Vertex2}}{\text{propagator}}, \quad (32)$$

where the vertex functions are in fact the partial widths of the resonance:

$$\text{vertex} = \Gamma_{R \rightarrow ab} \quad \text{and} \quad \Gamma_{R \rightarrow cd} \quad (33)$$

which can be expressed through the total hadronic width :

$$\Gamma_{R \rightarrow ab} = Br(R \rightarrow ab)\Gamma_{tot}. \quad (34)$$

When a relativistic resonance propagator is used, the vertex function becomes:

$$\text{vertex} \rightarrow \sqrt{m\Gamma} \quad (\text{for relativistic propagator}). \quad (35)$$

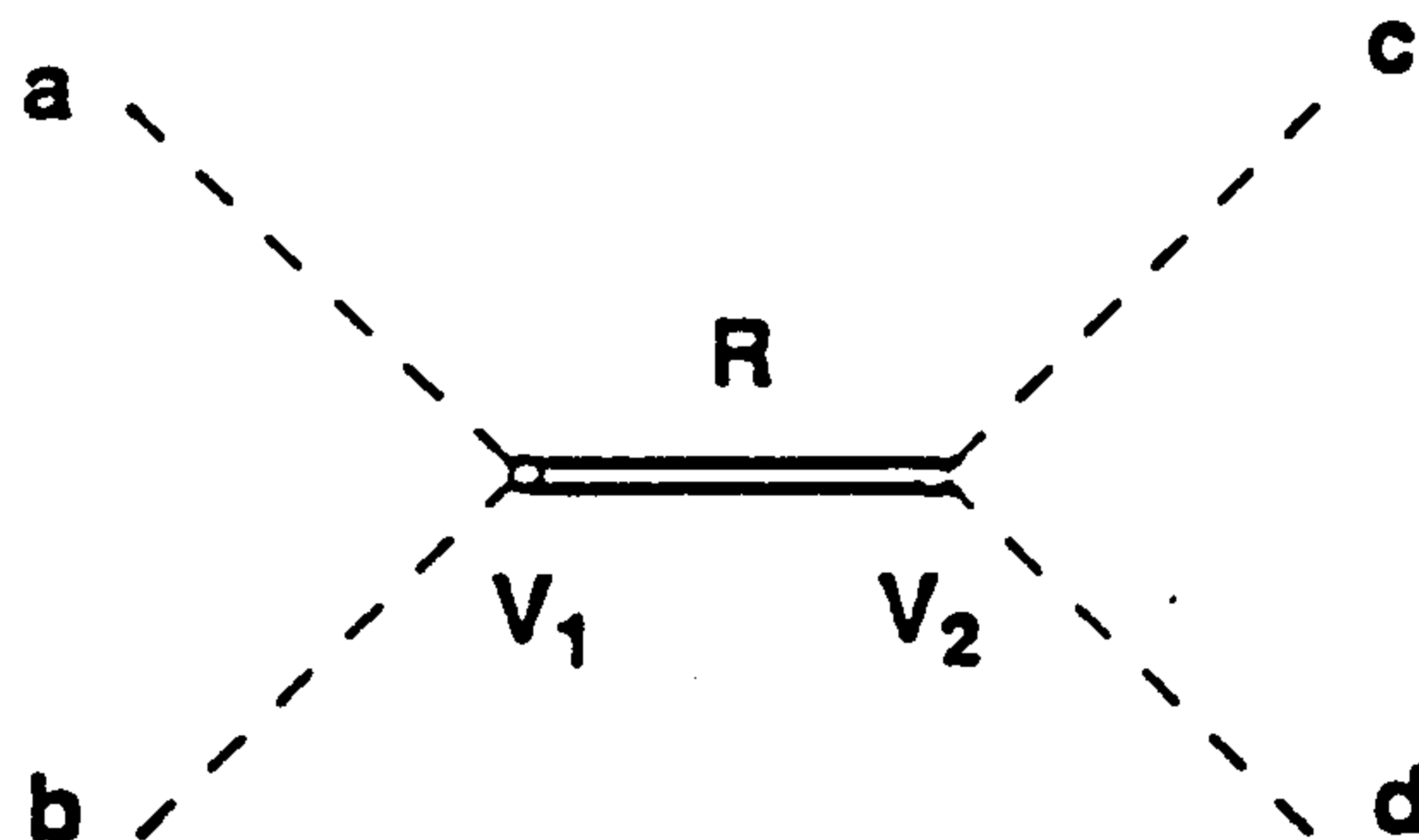


Figure 7: S channel resonance in two body scattering.

Therefore, for a reaction such as $e^+e^- \rightarrow ab$, Fig.2 (I), the partial wave amplitude is given by:

$$T \sim \frac{\sqrt{m_V\Gamma_1} \cdot \sqrt{m_V\Gamma_2}}{m_V^2 - m^2 - im_V\Gamma} = \frac{m_V\Gamma [B(V \rightarrow e^+e^-)B(V \rightarrow ab)]^{1/2}}{m_V^2 - m^2 - im_V\Gamma}. \quad (36)$$

For reactions such as $\gamma p \rightarrow abp$, Fig.2 (II), the partial wave amplitude will contain only one vertex function (the decay one) and therefore the Breit-Wigner form is given by :

$$T \sim \frac{\sqrt{m_V\Gamma_{V \rightarrow ab}}}{m_V^2 - m^2 - im_V\Gamma} = \frac{(m_V\Gamma)^{1/2} [B(V \rightarrow ab)]^{1/2}}{m_V^2 - m^2 - im_V\Gamma}. \quad (37)$$

The expression used for the analysis of the energy dependence of the $e^+e^- \rightarrow \eta\rho$ total cross section is given by:

$$\sigma = \frac{12\pi}{m^2} \left| G_{\rho_0} + \sum \eta_i G_{\rho_i} \right|^2 \quad (38)$$

and that for the $\eta\rho$ mass distribution from the reaction $\gamma p \rightarrow \eta\rho p$ is:

$$\frac{d\sigma}{dm} = \frac{2m}{\pi} \sigma(\gamma p \rightarrow \rho p) \left| F_{\rho_0} + \sum_i \xi_i \alpha_i F_{\rho_i} \right|^2 \quad (39)$$

with

$$\alpha_i = \left[\frac{\sigma(\gamma p \rightarrow \rho_i p)}{\sigma(\gamma p \rightarrow \rho_0 p)} \right]^{1/2} \quad (40)$$

and partial wave amplitudes of the the Breit-Wigner type :

$$G_\rho = \frac{m_\rho \Gamma_\rho}{m_\rho^2 - m^2 - im_\rho \Gamma_\rho} \left[B(\rho \rightarrow e^+ e^-) B(\rho \rightarrow f) \right]^{1/2} \quad (41)$$

$$F_\rho = \frac{1}{m_\rho^2 - m^2 - im_\rho \Gamma_\rho} (m_\rho \Gamma_\rho)^{1/2} B^{1/2}(\rho \rightarrow f). \quad (42)$$

The phase factors (the relative sign of the coupling constants) observed in Fig.6 in the interference pattern for $\eta\rho$ masses below 1.5 GeV requires a change in sign of the ρ' amplitude relative to ρ between photoproduction and e^+e^- annihilation, as was found earlier in ¹¹. In ref. ¹⁰ it was found that two classes of solutions are possible and they differ by the relative sign of the ρ components. These solutions are shown in Fig.6, (a and b) for the first solution and (c and d) for the second one.

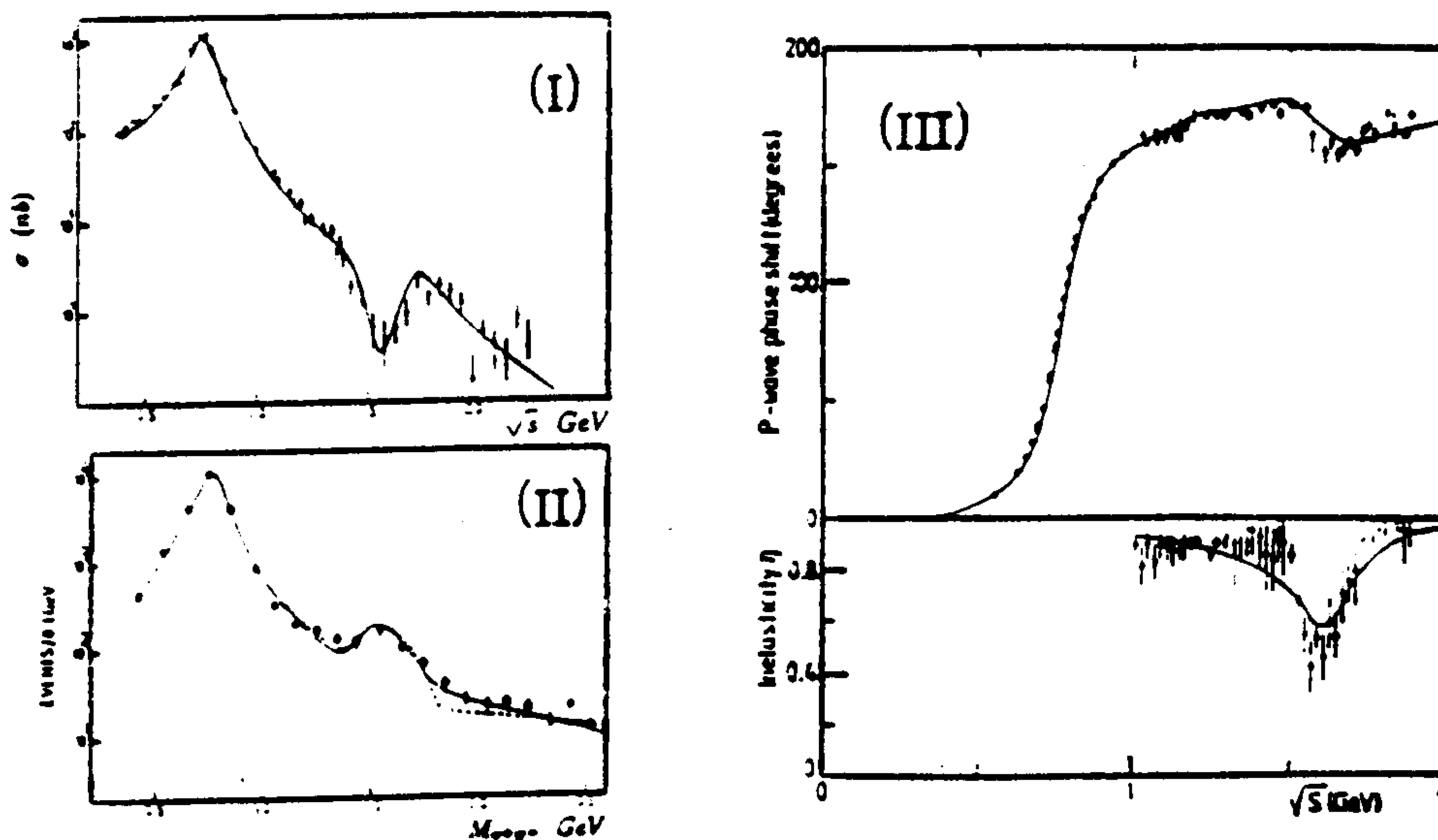


Figure 8: Fit of $e^+e^- \rightarrow 2\pi$ (I) , $\gamma p \rightarrow 2\pi$ (II) and fit of $(\pi\pi)$ P wave (III)

A more complex analysis of many different channels has been done by Donnachie and Mirzaie ¹¹ using experimental data on γp and e^+e^- having $\pi^+\pi^-$, $2\pi^+2\pi^-$ and $\pi^+\pi^-2\pi^0$ in the final state as well as the data on the phase shift and inelasticity for $\pi^+\pi^-$ scattering with $l=1$ (P wave). It was found that a good fit is obtained with two vector resonances with masses $M=1.465 \pm 0.025$ GeV, $M=1.700 \pm 0.025$ GeV and widths $\Gamma=0.235 \pm 0.025$ GeV and $\Gamma=0.220 \pm 0.025$ GeV respectively. The $(\pi^+\pi^-)$ branching ratio is 5 % for ρ_1 and 20 % for ρ_2 . Some results of this analysis are shown in Fig.10.

As is seen in Fig.8 (I and II) in the region of $m=1.5$ GeV there is a dip (e^+e^-) - bump (γp) structure which is resolved here by the sign changes of the relative phases (η_i and ξ_i in eq.38 and eq.39) between photoproduction and e^+e^- annihilation. The key feature in correlating all the data is the importance of 'off-diagonal' terms in photoproduction of states with $J^P=1^-$ and the contribution from states with $J^P \neq 1^-$.

It has been assumed and generally accepted that in applications of VDM the contributions of off-diagonal terms will be small and can be neglected. Now there is unambiguous evidence for diffraction dissociation of γ to states different of $J^P=1^-$. An example is the diffractive γ production of $b_1(1250)$ ($I^G(J^{PC}) = 1^+(1^{+-})$) which gives rise to the peak at 1.25 GeV in $\pi^+\pi^-2\pi^0$, Fig.5(I). There is also evidence for γ production¹⁷ of $h_1(1170)$ ($0^-(1^{+-})$) and $\rho_3(1690)$ ($1^+(3^{--})$). In the quark model these off-diagonal terms correspond to transitions of the type $1^3S_1 \rightarrow 1^1P_1$ or $1^3S_1 \rightarrow 1^3D_3$ and it is not unreasonable therefore to expect also :

- $1^3S_1 \rightarrow 2^3S_1$ for the lowest ρ radial excitation, and
- $1^3S_1 \rightarrow 1^3D_1$ for the lowest ρ orbital excitation.

The strong off-diagonal terms in photoproduction for higher ρ resonances destroys the simple VDM relations between phases and magnitudes of the amplitudes in photoproduction and e^+e^- annihilation. This effect is more evident in channels where the ρ tail is large (as in $\pi\pi$ final state where the dip-bump structure is observed. The relative phases $\rho:\rho':\rho''$ found in¹¹ are $++-$ in γp and $+ - +$ in e^+e^- (where there is a dip at $m=1.5$ GeV). Thus the sign of the $\rho'(1450)$ amplitude is negative in $e^+e^- \rightarrow \pi^+\pi^-$ and positive in $e^+e^- \rightarrow \eta\rho$. The coupling of a resonance to a final state is a signed quantity which cannot be fixed a priori and may have the same sign for different final hadronic states.

The analyses which are based on simple Breit-Wigner formulae do not satisfy the unitarity relation in the case of overlapping resonances. An analysis in which the explicit unitarised multichannel S-matrix is taken into account has been done by Hernner and Wolfson¹⁸. This analysis gives a good description of the $(\pi\pi)$ P-wave, and also the e^+e^- annihilation into 2π and 4π up to 2 GeV. The partial wave which describes the $(\pi\pi)$ system is written as a sum over all overlapping resonances:

$$f_{fi} = \sum_R \frac{m_R \Gamma_R B_{fR} C_{iR}^*}{m_R^2 - s - im_R \Gamma_R} \quad (43)$$

where B_{fR} is the decay branching ratio of the resonance R into the channel f. In the case of one resonance, C_{iR} is the usual branching ratio ($C_{iR} = B_{iR}$) and both B_{fR} and B_{iR} are real constants; the unitarity relations leads to $\sum_f B_{fi}^2 = 1$. In the case of overlapping resonances it is impossible to satisfy multichannel unitarity relations :

$$Im f_{fi} = \sum_n f_{fn}^* f_{ni} \quad (44)$$

if $C_{iR} = B_{iR}$. After lengthy algebra, an expression is obtained for the matrix C_{iR} which makes the partial amplitude satisfy the multichannel unitarity relations. The result of the fit provides evidence for three ρ states : at 1.25 GeV with $\Gamma=0.35$ GeV, at 1.61 GeV with $\Gamma=0.23$ GeV and at 1.8 GeV with $\Gamma=0.35$ GeV. An interesting conclusion is that, in spite of the possibility of obtaining good enough fits with the usual sum of Breit-Wigner terms, the results with and without unitarisation are substantially different.

Another important problem in analysing experimental data concerns the ρ (ω and ϕ) tail interference; the definition of the tail is somewhat model dependent. The simple approach (used earlier³⁷), taking the Breit-Wigner amplitude in the form :

$$BW \sim \frac{q^3}{m^2 - s - im\Gamma} \quad (45)$$

with Γ constant, turns out to be inadequate. The total width is in fact a sum of partial widths, each having an appropriate momentum dependence; a centrifugal barrier term, which depends on the radius of interaction R and is given by the so called Blatt-Weisskopf factor (or damping factor)²³. This is in fact a general problem of resonance amplitude parametrization which becomes important in the case of a broad resonance, for overlapping resonances and also in the case of a resonance with a mass very near to a threshold. For the case of ρ P wave decay ($l=1$), the simple $q^{(2l+1)}$ momentum dependence of the partial width changes:

$$q^3 \longrightarrow q^3(1 + (qR)^2)^{-1}. \quad (46)$$

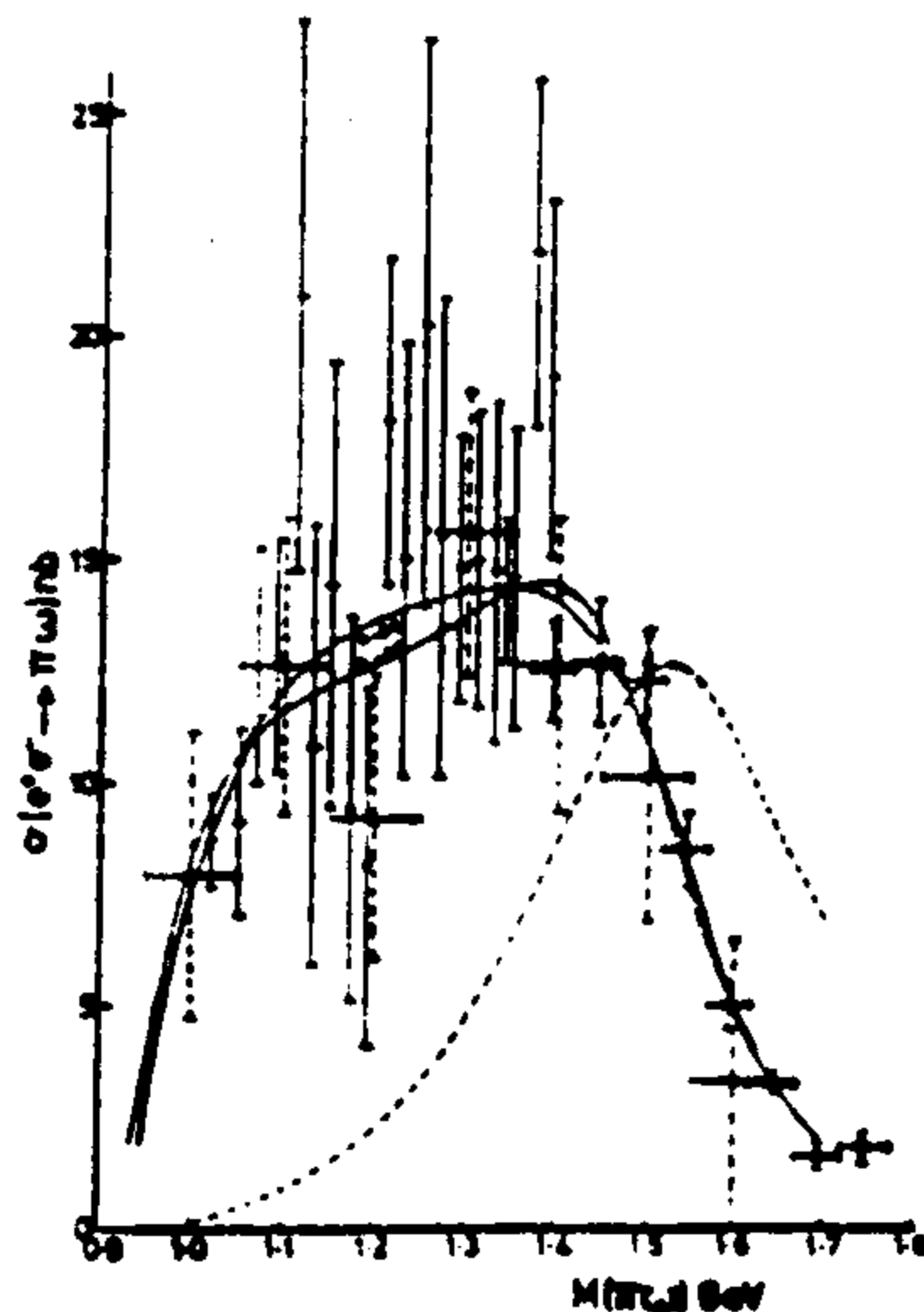


Figure 9: Typical fits of $e^+e^- \rightarrow \omega\pi$. Full curves include ρ' and a ρ tail with $R=0.2, 0.8$ fm; the dashed curve shows the ρ' contribution.

Using these modifications, the analysis³⁷ of $e^+e^- \rightarrow \omega\pi$ shows a strong correlation between the mass of the ρ' and R ; the mass is largest when R is small, but compatible with previous results (a mass in the range 1.46 to 1.50 GeV and the width in the range 0.34 to 0.40 GeV). There is no need for the second ρ'' ; the interference found is the canonical (+ -) and the parameter R is in the range 0.0 to 0.8 fm, Fig. 9.

Information on the vector mesons can also be obtained from the analysis of the electromagnetic form factors. In the VDM framework, all the electromagnetic form factors are completely dominated by the contribution of the ρ , ω , and ϕ mesons. Neglecting the G parity violating transitions (which allow transitions of ω and ϕ into 2π), the pion electromagnetic form factor is given by the main ρ contribution:

$$F_\pi = \frac{g(\rho\gamma)g(\rho\pi\pi)}{D(\rho)} \quad (47)$$

where $D(\rho)$ is the ρ meson propagator given by:

$$D(\rho) = s - m_\rho^2 + i \frac{m_\rho^3}{2} \Gamma_\rho \left(\frac{s - 4m_\pi^2}{m_\rho^2 - 4m_\pi^2} \right)^{3/2} \quad (48)$$

and with pion coupling constant

$$g(\rho\gamma)g(\rho\pi\pi) = 0.705 \pm 0.089 \text{ GeV}^2. \quad (49)$$

The analysis of the pionic form factor in the region $1.34 < \sqrt{s} < 2.4$ GeV by the DM2 Collaboration²⁰ shows that the experimental data are not compatible with the simple VDM, even when adding the interfering contribution of an excited ρ' . The mass

obtained from this last fit is $m_{\rho'} = 1.73 \pm 0.02$ GeV, $\Gamma_{\rho'} = 0.11 \pm 0.02$ GeV with a $\chi^2/N_{dof} = 43.3/13$. The fit is improved (to $\chi^2/N_{dof} = 19.9/8$) if three ρ resonances are permitted to interfere, Fig.10:

$$F_{\pi} = \sum_{k=0}^2 g_k(\rho\gamma)g_k(\rho\pi\pi) \frac{1}{D_k(\rho)} e^{i\phi_k}. \quad (50)$$

Fixing the phase of the fundamental $\rho(770)$ to zero, the relative phases for the first and the second ρ recurrence are :

$$\phi_1 = 3.14 \pm 0.025 \text{rad} \rightarrow \pi \quad (51)$$

$$\phi_2 = 0.004 \pm 0.06 \text{rad} \rightarrow 0, \quad (52)$$

confirming experimentally the so called 'canonical phases' (+ - +) found before by Donnachie¹¹. The masses and the widths are $m=1.424$ GeV , $\Gamma=0.269$ GeV and $m=1.768$ GeV , $\Gamma=0.224$ GeV for ρ' and ρ'' respectively.

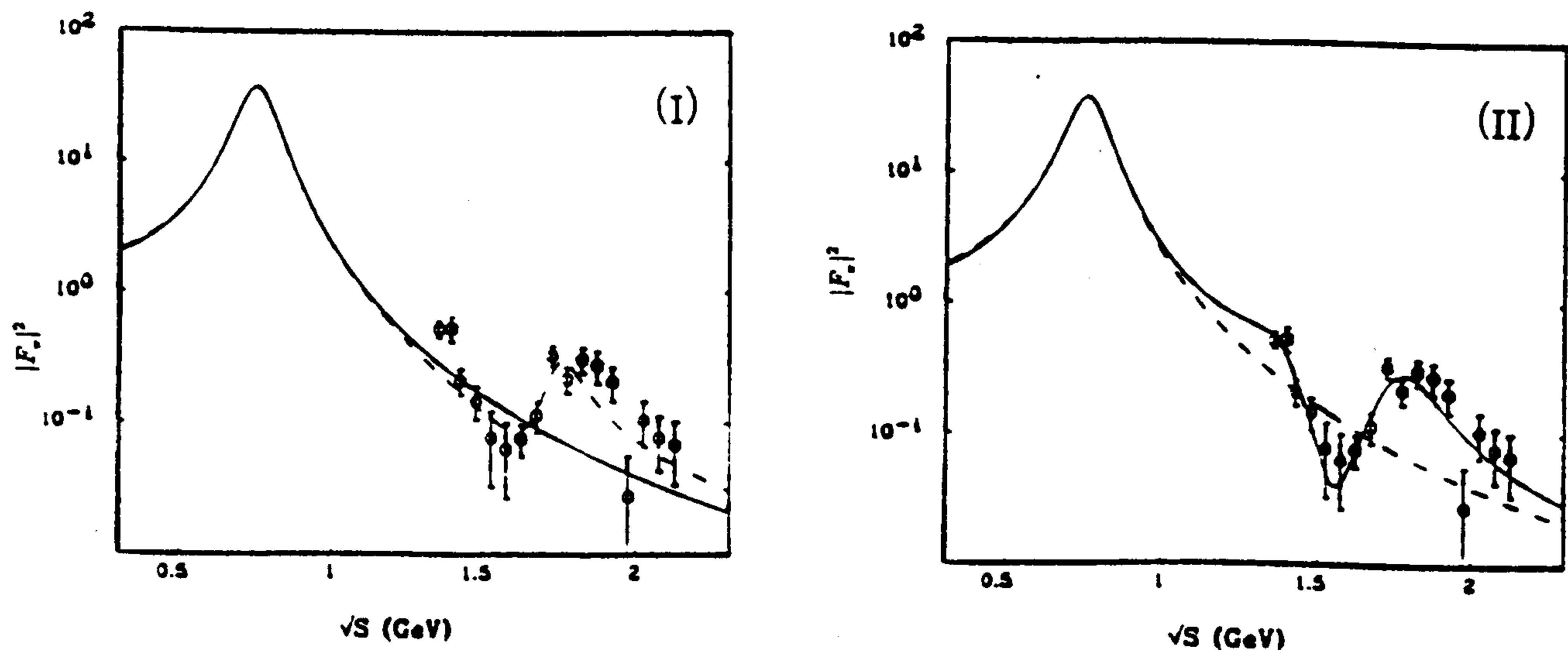


Figure 10: The fit of the pion squared form factor with a single ρ' interfering resonance (I), and with two ρ' interfering resonances (II). The tail of $\rho(770)$ is also shown.

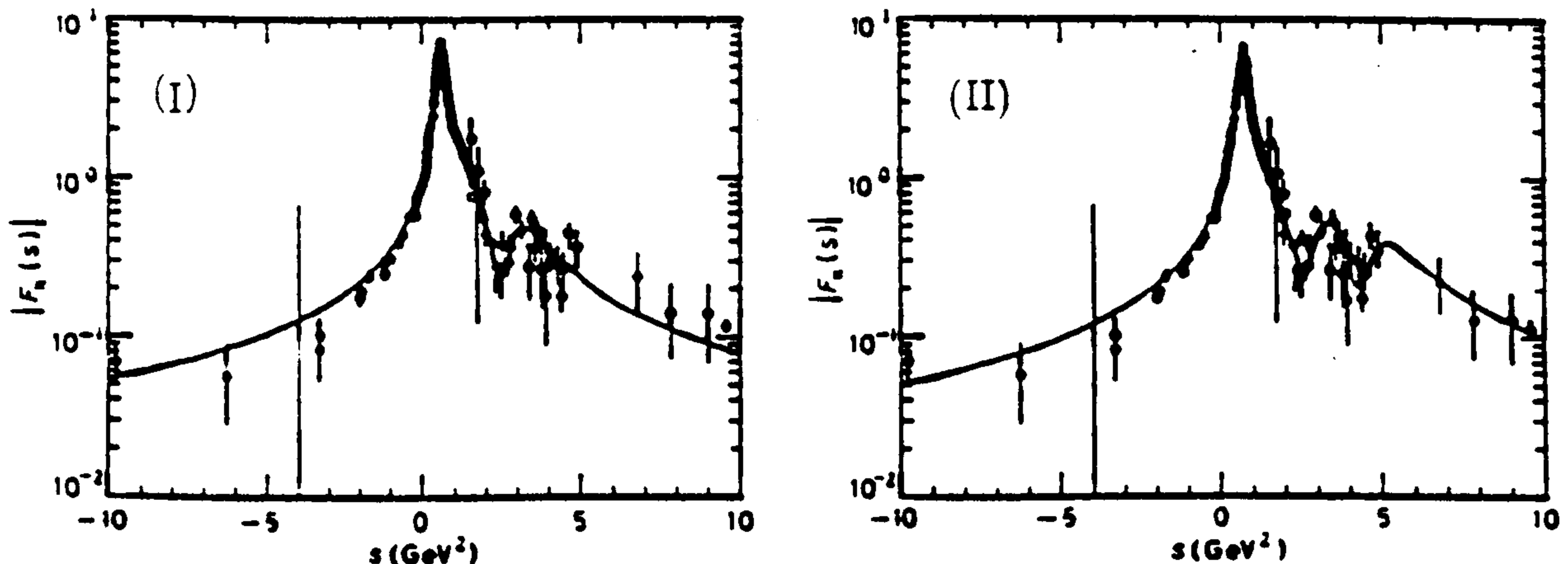


Figure 11: Fit of the modulus of the pion form factor with $\rho(770)$, $\rho'(1450)$ and $\rho''(1700)$ (I) and a fit with three excited states, as before and $\rho'''(2150)$ (II).

A more complex study of the pionic form factor (using in the fit data on space-like as well as time-like regions, but also some data on kaonic form factors) confirms the existence of two ρ excited states at 1.45 GeV and 1.70 GeV. This phenomenological

analysis also shows there is a case for the existence of a third excitation of $\rho(770)$ with mass $m=2.15$ GeV and width $\Gamma=0.320$ GeV, Fig.11; this points to the same structure identified by Clegg and Donnachie²² in an analysis of electron positron annihilation into 6π . This third ρ excited state has also been observed by the GAMS Collaboration in a study of the $\omega\pi^0$ system produced in the π^-p charge exchange reaction at 38 GeV/c. The OPE mechanism limits the quantum numbers of the $\omega\pi^0$ system to the following $J^{PC} = 1^{--}, 3^{--}, \dots$ and $I^G = 1^+$. The X(2200) observed in ref.²⁴ is confirmed in ref.²⁵ to be a 1^{--} state, the $\rho(2150)$; this may be a radial-orbital excitation belonging to the 2^3D_1 nonet with mass and width $m=2.140 \pm 0.030$ GeV, $\Gamma = 0.320 \pm 0.070$ GeV. In conclusion, the sector of isovector vector mesons contains two broad ρ excited states, the first one $\rho(1450)$ with $\Gamma=0.310$ GeV belonging to the 2^3S_1 nonet and a second one $\rho(1700)$ with $\Gamma=0.235$ GeV belonging to 1^3D_1 nonet. There is also evidence for states around $m=2.00$ GeV and $m=2.15$ GeV, possible 3^3S_1 and 2^3D_1 states.

4. Isoscalar and strange vectors

4.1. Isoscalar ω states.

In this sector it is highly probable that there is a strong ($\omega' - \phi'$) mixing, so the notation of these states as ω' or ϕ' is not so straightforward. There is also the possibility of there being isoscalar hybrid states which can also confuse the situation. The study of ω' states is made on data $e^+e^- \rightarrow \rho\pi$ and $e^+e^- \rightarrow \omega\pi\pi$. These data show a very different behaviour, the second one dominating at 1.6 GeV.

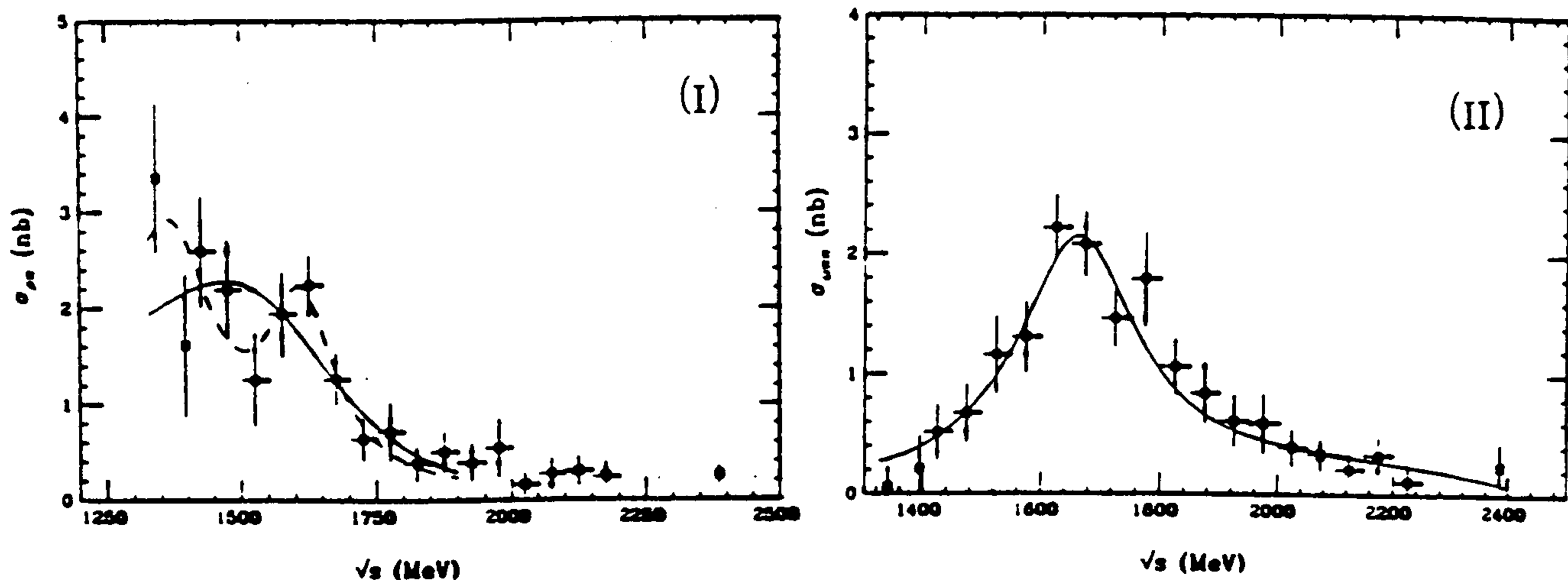


Figure 12: Cross section for $e^+e^- \rightarrow \rho\pi$ (I) and $e^+e^- \rightarrow \omega\pi\pi$ (II).

If one follows the conventional view of the ρ' excitations, then in fitting the data it is natural to take into account one or two new states. From the fit of the experimental data³⁷ on $\rho\pi$ two ω states are required with so called 'canonical phases', $\omega : \omega' : \omega'' = (+ - +)$. The masses and widths of the ω excited states are $m=1.44$ GeV, $\Gamma=0.24$ GeV for the first and $m=1.60$ GeV, $\Gamma=0.140$ GeV for the second. However, the data are also compatible with only one ω' at $m=1.635$ GeV and $\Gamma=0.350$ GeV. The $\omega\pi\pi$ final state exhibits only one clear resonant peak at $m=1.598$ GeV with $\Gamma=0.109$ GeV¹⁹.

A more recent analysis of new experimental data²⁶ gives practically the same values of masses and widths as the previous analyses (in Fig.12, the continuous line in (I) is a single Breit-Wigner fit of the $\rho\pi$ final state).

Because the fits above 1.6 GeV for electron positron annihilation to $\rho\pi$ and $\omega\pi\pi$

are similar, a coupled fit of both types of data has also been performed giving $m=1.662$ GeV and $\Gamma=0.280$ GeV. The large cross section in $\omega\pi\pi$ suggests that this state is of ω type (mainly non strange quarks).

The first ω' , seen only in the $\rho\pi$ final state is unstable due to the experimental problems (cross section normalization). The present status of the isoscalar ω type vector mesons is illustrated by the PDG⁷. The first state is $\omega(1420)$, belong to the first radial excitation (2^3S_1 nonet), decaying dominantly to $\rho\pi$; it has mass and width $m=1.419 \pm 0.031$ GeV, $\Gamma=0.174 \pm 0.060$ GeV. The second one, $\omega(1600)$, belonging to the first orbital nonet (1^3D_1), decays to $\rho\pi$ and $\omega\pi\pi$ and has the parameters: $m=1.662 \pm 0.013$ GeV, $\Gamma=0.280 \pm 0.024$ GeV.

4.2. Isoscalar ϕ states.

Data used for ϕ' observations are from photoproduction reactions with two kaons in the final state:

$$\gamma p \longrightarrow K \bar{K} X \quad (53)$$

as well as from electron positron annihilation :

$$e^+e^- \longrightarrow K^+K^- \quad (54)$$

$$e^+e^- \longrightarrow K_S K_L \quad (55)$$

$$e^+e^- \longrightarrow K^* \bar{K}. \quad (56)$$

The photoproduction mechanism is found to conserve s-channel helicity and to proceed via natural-parity exchange in the t-channel²⁷. From the analysis of photoproduction data, only one resonant state is found in the mass region of 1.7 GeV. The values found in two important analyses are in agreement : $m=1.760 \pm 0.020$ GeV, $\Gamma=0.080 \pm 0.040$ GeV²⁷ and $m=1.726 \pm 0.022$ GeV, $\Gamma=0.121 \pm 0.047$ GeV²⁸.

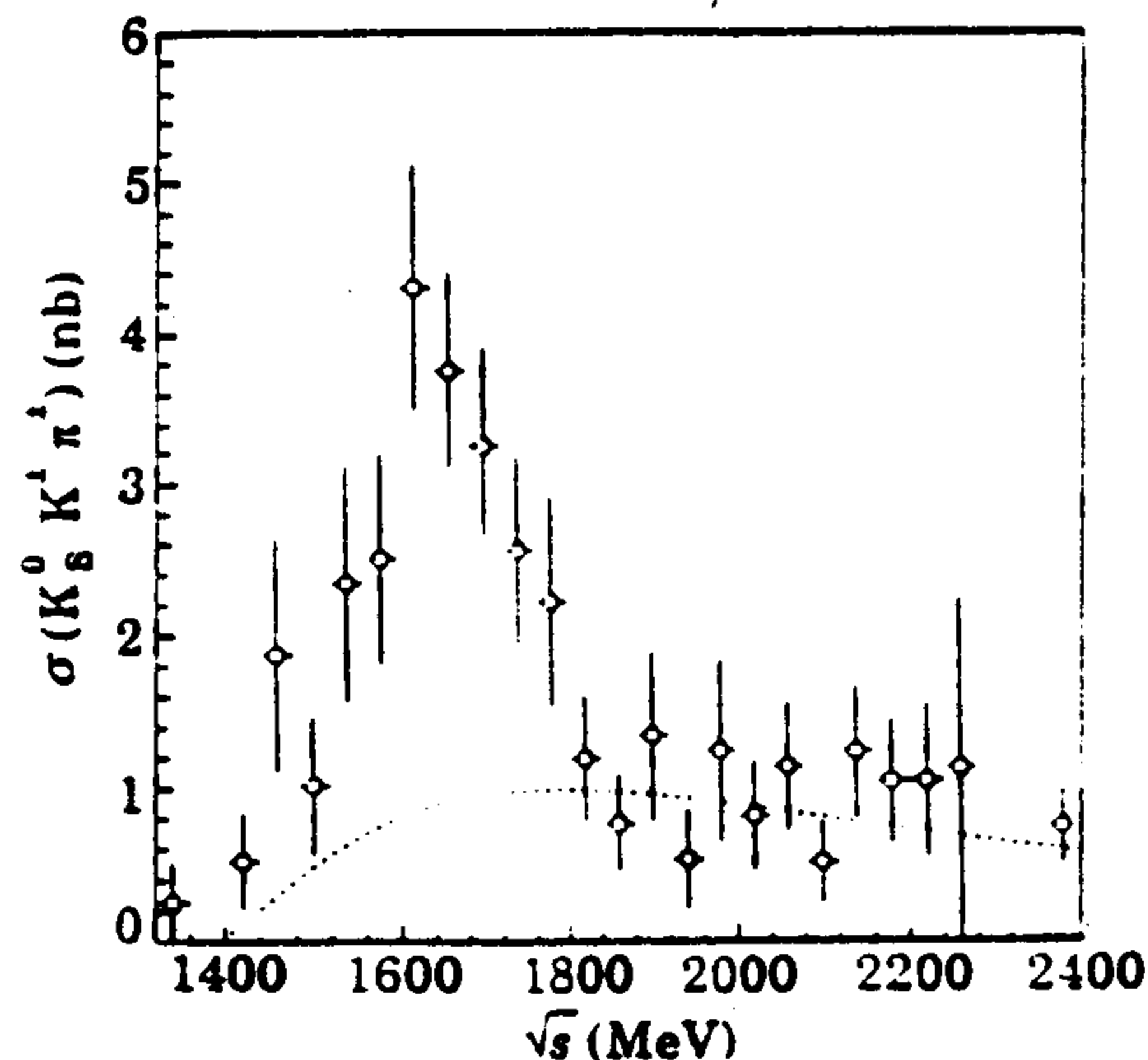


Figure 13: Cross section for $e^+e^- \longrightarrow K_S^0 K^\pm \pi^\mp$.

The analysis of e^+e^- annihilation shows also only one resonant state in $K\bar{K}$ but with parameters slightly different: $m=1.655 \pm 0.017$ GeV, $\Gamma=0.207 \pm 0.045$ GeV²⁹. The cross section for e^+e^- annihilation into three bodies (Eq.56) shows an enhancement around 1.650 GeV which cannot be explained simply by the contributions of only ρ , ω and ϕ (the dashed line in fig.13). A maximum likelihood fit to the Dalitz plot requires a clear $K^*(892)K$ dynamics with K^*0 dominance; this indicates an interference between a weak isovector (ρ like) and a resonant isoscalar (ϕ like) amplitude. Figs.14 (a) and (b).

The relative phase as well as the absolute isoscalar phase (assuming for ρ' $m=1.57$, $\Gamma=0.51$ GeV) is found to cross 90° in the same mass region where the peak in the cross section is observed; this supports a resonant nature for the observed signal, Figs.14 (c) and (d). The mass and width values found are $m=1.657 \pm 0.027$ GeV and $\Gamma = 0.146 \pm 0.055$ GeV. This result, in close agreement with other measurements, supports the identification of this isoscalar vector meson decaying mainly to $K^*\bar{K}$; this $\phi'(1680)$ is the first radial excitation of ϕ (2^3S_1 nonet).

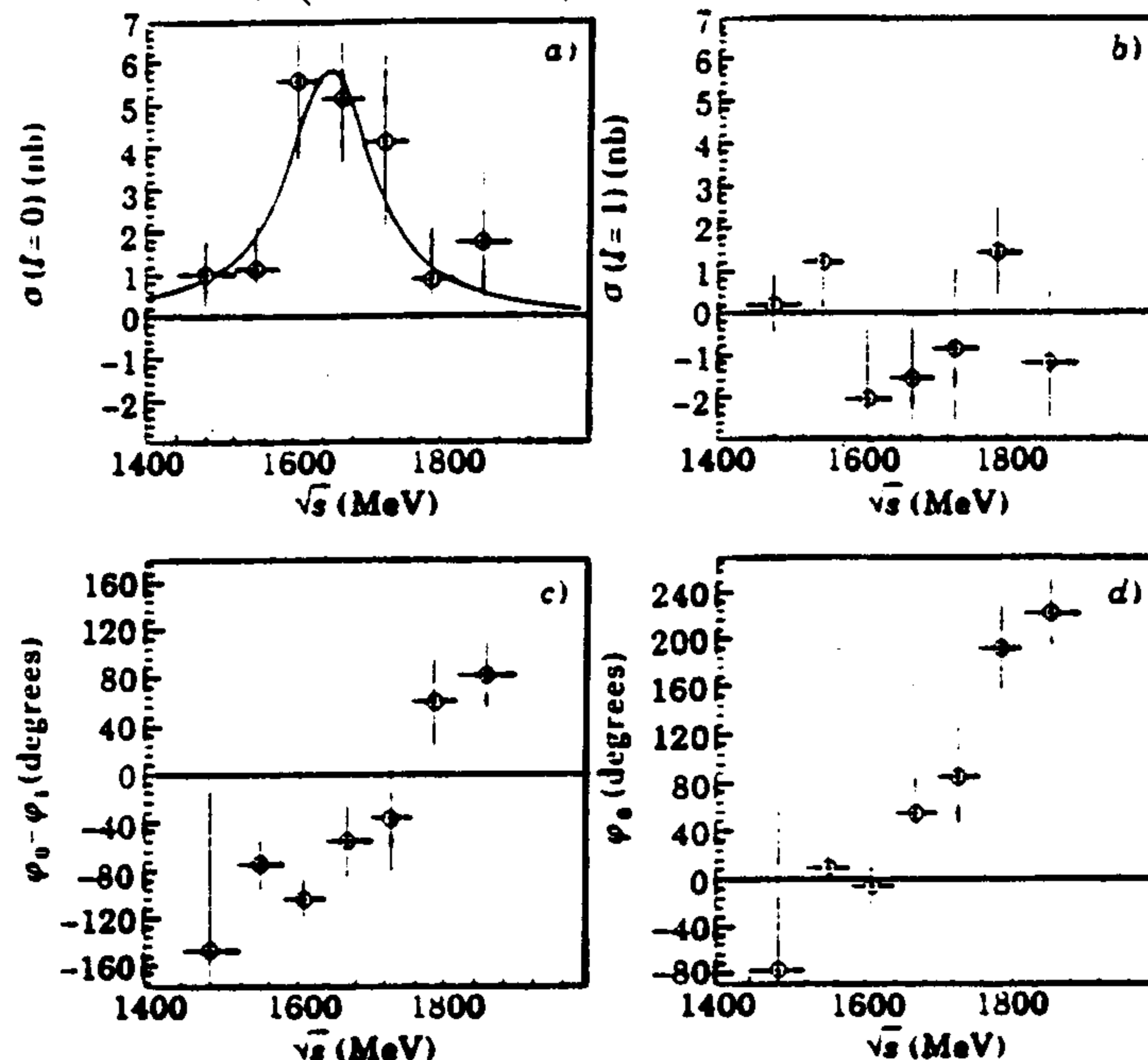


Figure 14: The Dalitz plot analysis of $K_S^0 K^\pm \pi^\mp$. Isoscalar (a) and isovector (b) cross sections, relative phase between them (c) and absolute isoscalar phase (d).

4.3. Strange vectors.

The strange vectors appear to be an ideal place to study $(q\bar{q})$ spectroscopy due to the absence of glueballs and absence of isoscalar mixing. The $(K\pi)$ and $(K\pi\pi)$ systems can be produced in both diffractive and charge-exchange reactions. The $(K\pi)$ provides information on natural spin-parity amplitudes. The $(K\pi\pi)$ systems produced diffractively is dominated by unnatural spin-parity states and by natural ones in charge-exchange production.

In this sector of strange 1^- mesons, the main results come from the LASS collaboration at SLAC ^{31,32}. The reactions analysed are $K^-p \rightarrow K\pi(n/p)$ and $K^-p \rightarrow K\pi^+\pi^-n$.

The 1^- partial waves arise from the production and decay of two states. The lower in mass decays mostly to $K^*\pi$. The mass and width averaged over three measurements of three final states ($\bar{K}^0\pi^+\pi^-$, $K^-\pi^+$ and $\bar{K}^0\pi^-$) are $m=1.412 \pm 0.012$ GeV and $\Gamma=0.227 \pm 0.022$ GeV (average given by ref.⁷).

The second state decays almost equally to $K\pi$, $K^*\pi$ and $K\rho$ and has mass and width $m=1.714 \pm 0.020$, $\Gamma = 0.323 \pm 0.110$ GeV (as given in ref. ⁷).

Fig.15 shows the $K^*\pi$ and $K\rho$ 1^- contributions from the partial wave analysis of $K\pi\pi$ production. The curves are the result of a simultaneous two resonance fit to 1^- waves and K^* in the 2^+ and 3^- waves including their relative phases. The phases are set using the predicted behaviour of the $(K^*\pi)_P$ reference wave, Fig.15 (c).

It is therefore natural to associate the first 1^- state $K^*(1410)$ with the first radial excitation of the $K^*(890)$ (the 2^3S_1 nonet) and the second one, $K^*(1680)$ with the first

orbital excitation (the 1^3D_1 nonet).

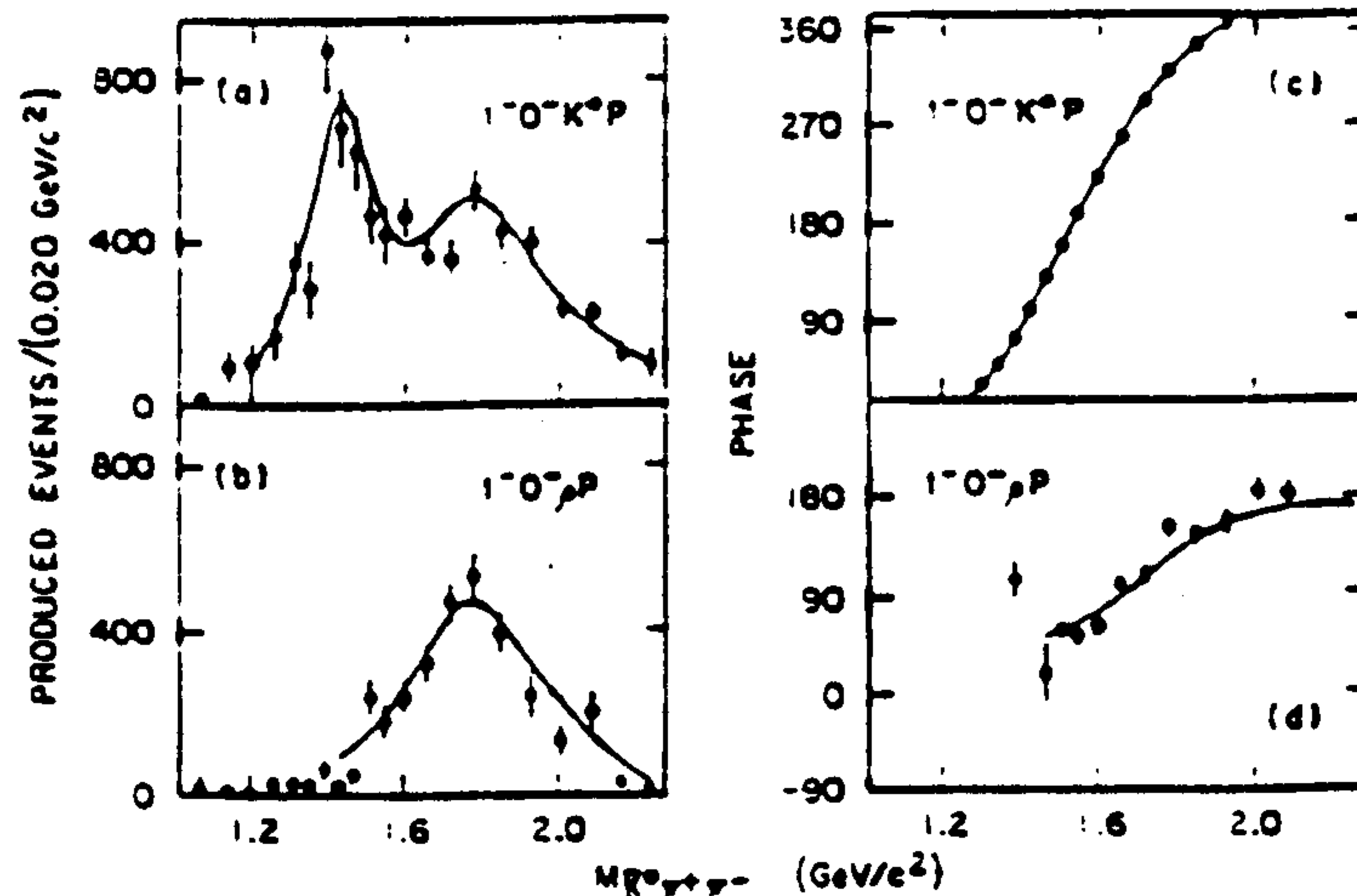


Figure 15: Fit of 1^- waves from $K^-p \rightarrow K\pi^+\pi^-n$.

5. Exotica ?

The low mass $\rho'(1300)$ has been claimed many times (in PDG 86⁹ it is mentioned as $\rho(1250)$) but never generally accepted. We recall here the analysis with unitarised amplitudes¹⁸, some evidence for it in $\pi\pi$ spectra³⁴ and of J/Ψ decay in $\pi^+\pi^-\pi^0$; the recent LASS analysis³³ of $K^-p \rightarrow \pi^+\pi^-\Lambda$ found the parameters $m=1.302 \pm 0.028$ GeV and $\Gamma=0.140 \pm 0.048$ GeV. Fig.16 shows the magnitude of the P wave and its phase motion relative to the D wave (fixed to $f_2(1270)$ parameters). The solid curve is the fit with ρ , ω - ρ interference and $\rho'(1300)$. The dotted curve shows the effect of omitting $\rho'(1300)$.

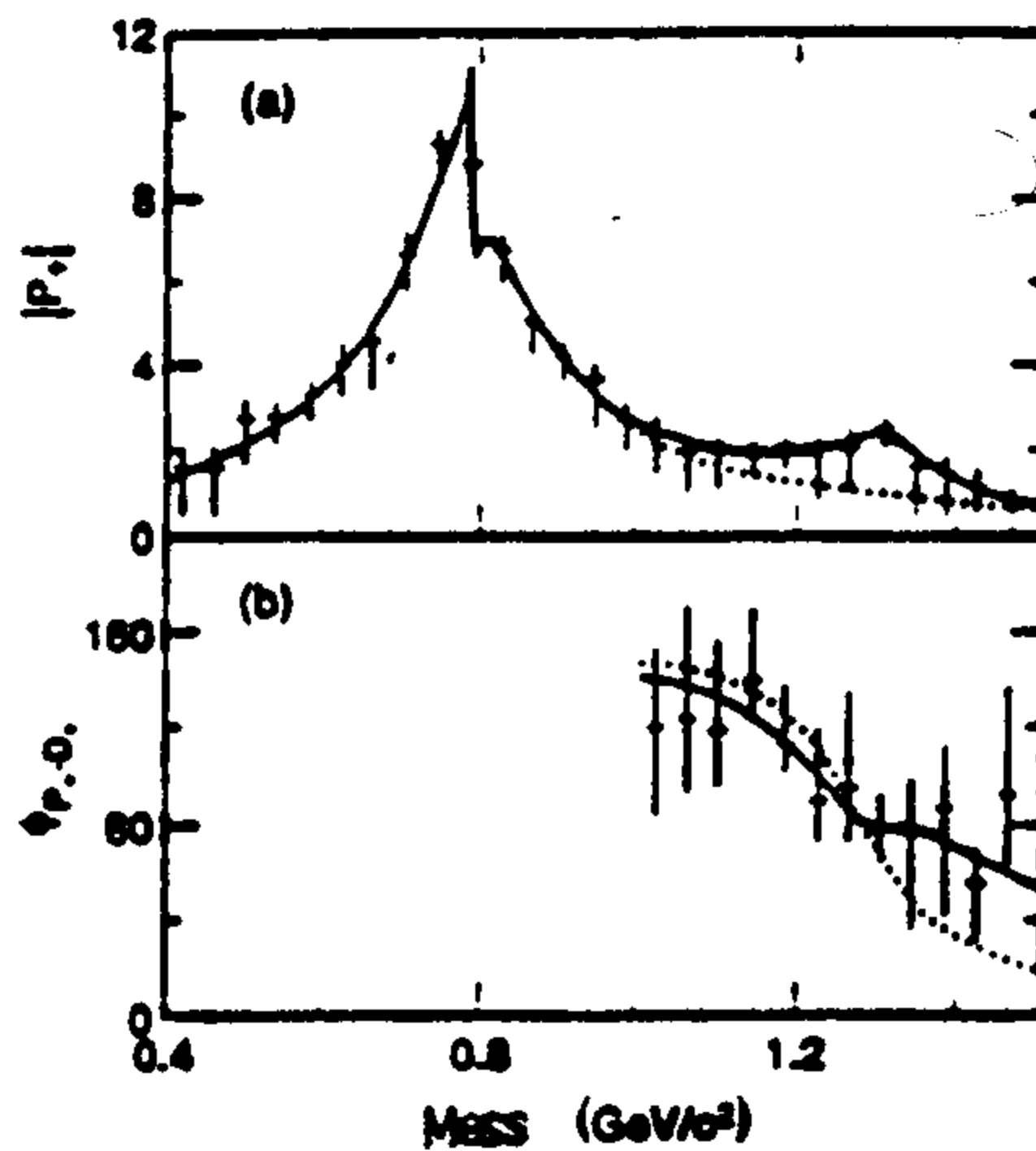


Figure 16: The magnitude and the relative phase of P wave from the reaction $K^-p \rightarrow \pi^+\pi^-\Lambda$

The problem is therefore the number of ρ' states in the region 1.25 - 1.5 GeV and, if we accept two states, which is the partner of $K^*(1410)$?

A possible explanation was given in ref. ³⁸. Invoking the concept of $q^2\bar{q}^2$ states coupled to the normal $q\bar{q}$ mesons, a mixing scheme is proposed in which both ρ' exist, at $m=1.45$ GeV and at $m=1.270$ GeV, one being built mostly of $q^2\bar{q}^2$. Anyway, if there are indeed two ρ' states in the mass region of 1.3 to 1.45 GeV, from ref. ³⁹ the lower one can be an 'almost multiquark state' and from ref. ⁴⁰ the heavier one can be a 'possible hybrid state'.

Another candidate for exotica in the vector meson sector can be the so-called C(1480) meson, seen for the moment only in one experiment³⁵ in the reaction $\pi^- p \rightarrow \phi\pi$. The mass and width are found to be $m=1.480 \pm 0.04$ GeV and $\Gamma = 0.160 \pm 0.06$ GeV with the quantum numbers $1^+(1^{--})$ (just like the ρ meson).

The coincidences of the mass of C(1480) with those of the ρ' raises the problem of whether these can be different observations of the same vector meson. The identification of a strong ρ' decay in $\omega\pi$ and the analysis of different partial widths of the 1.45 GeV resonant structure^{36,37} supports the claim that the ρ' and C(1480) cannot be the same particle. So, if C(1480) is confirmed by other experiments it can be a candidate for an extra vector meson, a possible signature of exotica in this sector.

The most obvious signature for an exotic meson is in fact the existence of an object with an exotic combination of J^{PC} , for example a 'vector meson' with positive C parity (1^{-+}) (so called $\hat{\rho}$ states).

The simplest system where exotic J^{PC} states can be sought is $\eta\pi$ in odd angular momentum between η and π . Such states were claimed around $m=1.400$ GeV in $\eta\pi$ invariant mass from the analysis of the reaction $\pi^- p \rightarrow \pi^0\eta n$ at 100 GeV/c ($m=1.406 \pm 0.020$ GeV, $\Gamma = 0.180 \pm 0.030$ GeV)⁴¹ and of reaction $\pi^- p \rightarrow \pi^- \eta p$ at 6.3/c GeV/c ($m=1.323 \pm 0.005$ GeV, $\Gamma = 0.143 \pm 0.016$ GeV)⁴². From the partial wave analysis, in spite of possible ambiguities^{43,44} (eight solutions for a S,P,D analysis), both experiments found a clear signal of a well known $a_2(1320)$ (D wave), an enhancement of the P wave and an almost flat D-P relative phase, Fig.17⁴², (which means that both waves are resonant or both non-resonant).

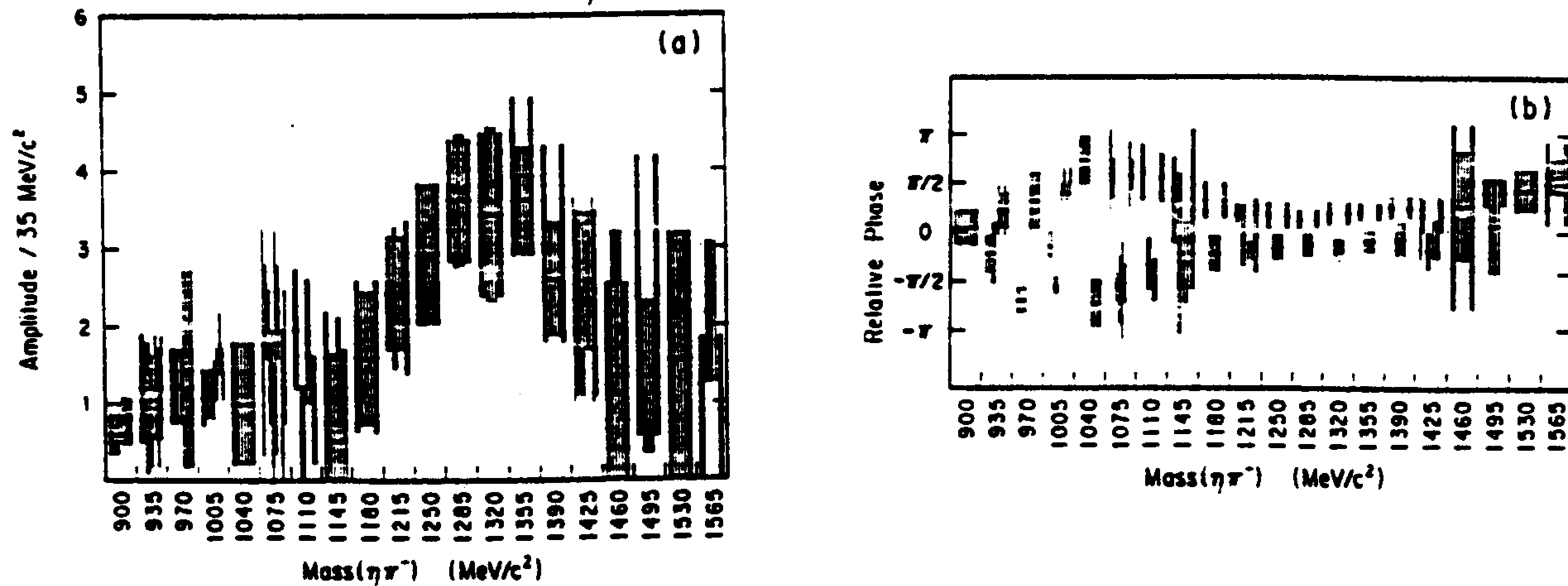


Figure 17: Distribution of amplitudes of the P wave (a) and relative D-P phase (b). Eight solutions are plotted adjacently.

In a recent study⁴⁵ of the reaction $\pi^- p \rightarrow f_1(1285)\pi^- p$ at 18 GeV/c (with $f_1(1285) \rightarrow K^+ \bar{K}^0 \pi^-$), an exotic signal was also found in the $f_1(1285)\pi$ invariant mass, a broad 1^{-+} structure ($f_1\pi$ in S wave) at 1.6-2.2 GeV.

The limited statistics and the existence of ambiguities in the partial wave analysis implies that all these observations need urgently confirmation.

6. Discussion.

The first simple linear dependence in m^2 which correlates the mass and the spin of the resonances was the Regge trajectory :

$$m^2 = aJ + b_1. \quad (57)$$

This relation is suitable for examining the systematics of the isovector states because they do not suffer from hidden strangeness admixture and have bigger production cross

sections than others. For the natural spin-parity series, the leading trajectory (leading means that the corresponding states have the lowest known m^2 for each spin J) is given by the parameters ²⁵: $a = 1.16 \pm 0.04 \text{ GeV}^2$ and $b = -0.56 \pm 0.05 \text{ GeV}^2$, Fig.18.

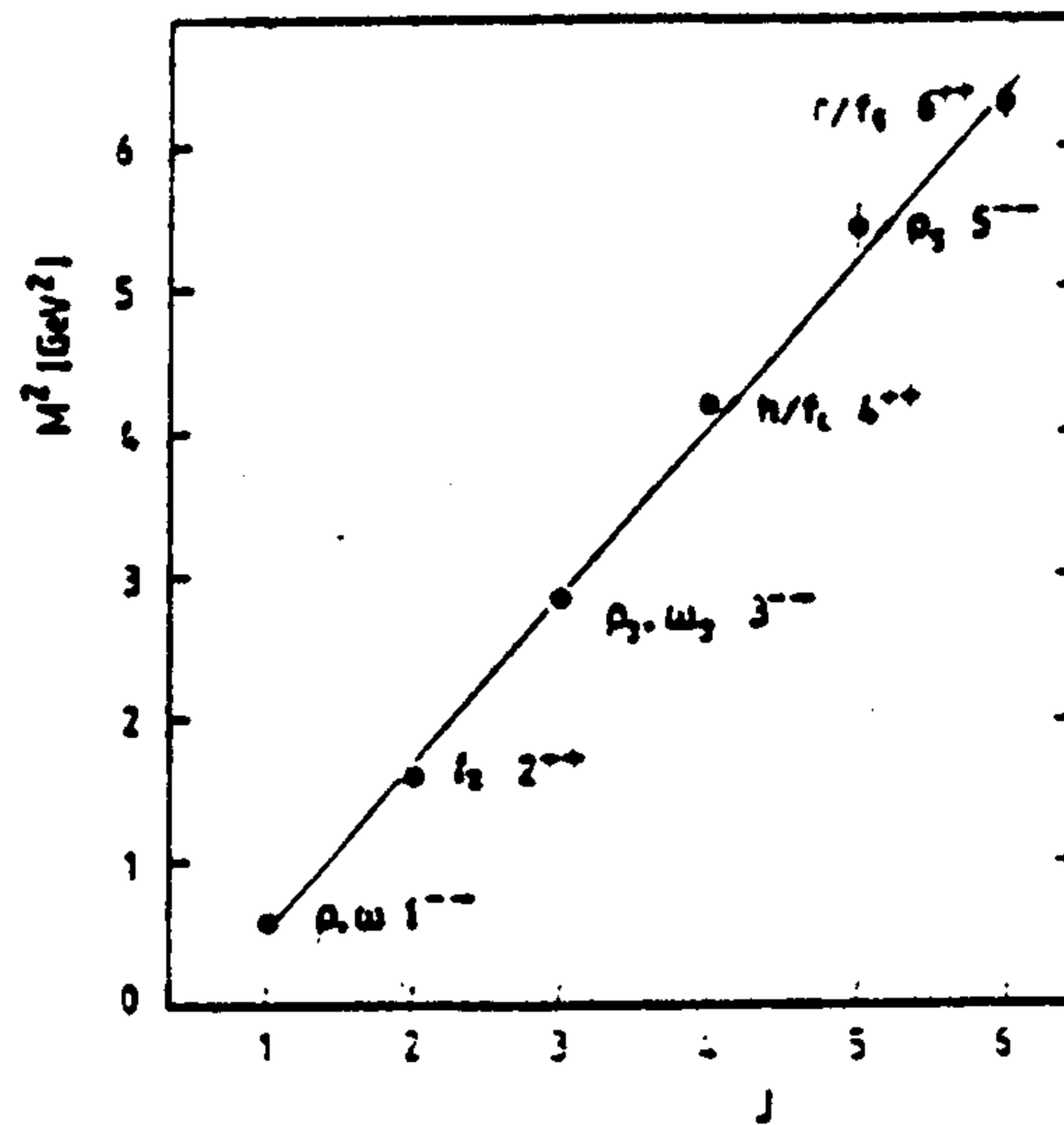


Figure 18: Regge trajectory for normal spin-parity series.

For the radial excitations we can expect a similar trajectory, with the same slope but with a displacement in b ($b_n > b_1$). Indeed, the Veneziano ⁴⁶ formula gives a relation for b_n :

$$b_n = an + b_0 \quad (58)$$

where 'a', to first order is the same as before. Therefore the Veneziano-Regge formula useful also for excited states has the general form ⁴⁷:

$$m^2 = an + b(I^G, J^{PC}) \quad (59)$$

which means a linearity in excitation number. Such a dependence is shown for the vector mesons in Fig.19²⁴ in which, as a curiosity, we indicate by an arrow the position of $\rho'(1.300)$ at $m = 1.32 \pm 0.04 \text{ GeV}$.

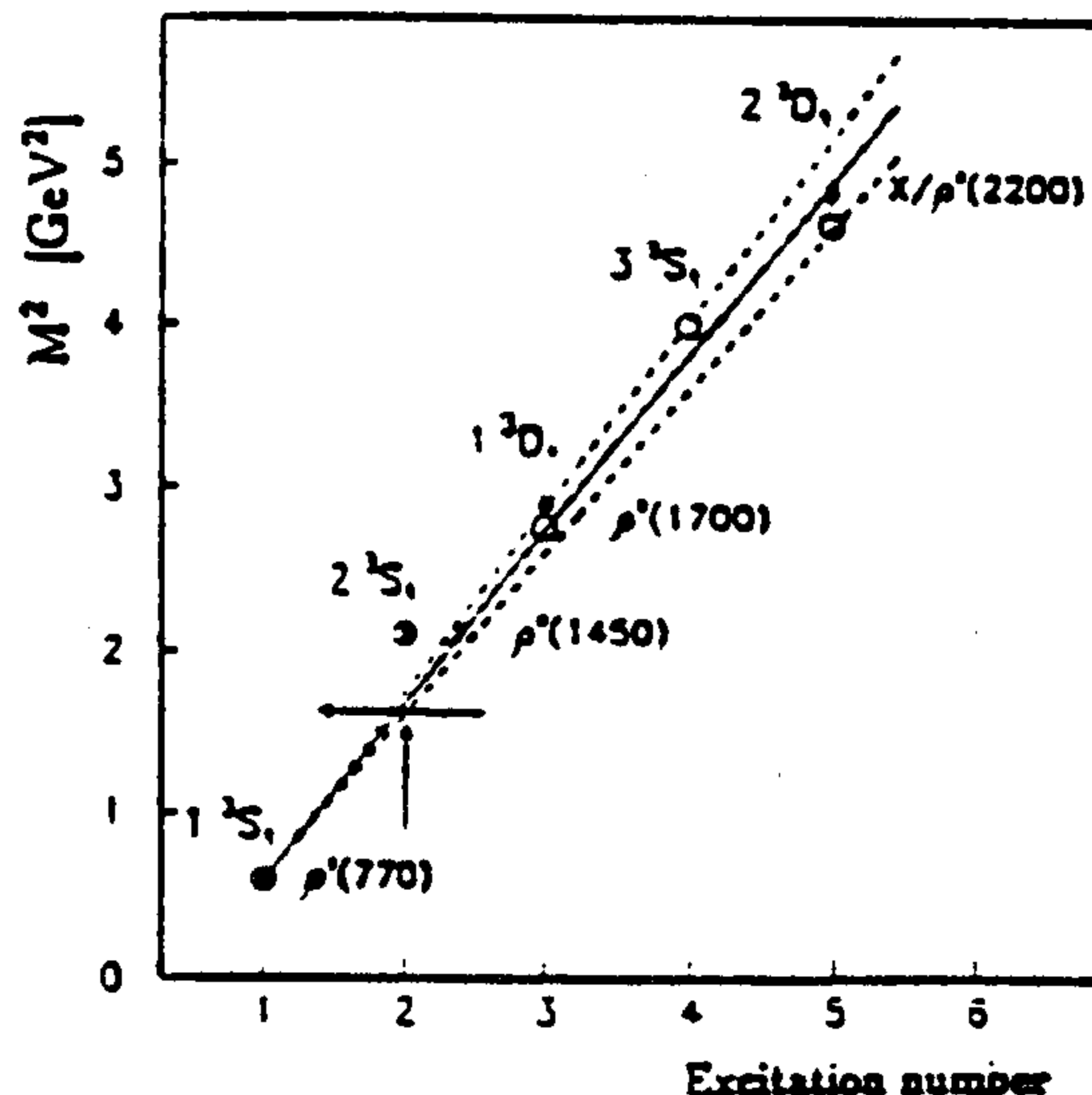


Figure 19: Excitation trajectory for vector mesons. Dots are experimental values and open circles are Godfrey-Isgur predictions.

The present status of the vector mesons composed by light quarks can be summarized in the table shown below, where for completeness we add also higher J states.

J^{PC}	$I = 1$	$I = 0$		$I = 1/2$
1^3S_1 1^{--}	$\rho(770)$	$\omega(782)$	$\phi(1024)$	$K^*(892)$
2^3S_1 1^{--}	$\rho' \begin{matrix} \swarrow (1.30) \\ \searrow (1.45) \end{matrix}$	$\omega'(1420)$	$\phi'(1680)$	$K'^*(1410)$
3^3S_1 1^{--}	1.8 – 2.15	?	?	?
1^3D_1 1^{--}	$\rho''(1700)$	$\omega''(1600)$?	$K''^*(1680)$
2^3D_1 1^{--}	2.20	?	?	?
3D_3 3^{--}	$\rho_3(1690)$	$\omega_3(1670)$	$\phi_3(1850)$	$K_3(1780)$
3G_5 5^{--}	2.35	?	?	$K_5(2380)$
1^{-+}	$\hat{\rho}(1400)$		$\hat{\rho}(2000)$	

The first order problem in this sector is the correct filling of the nonets in order to be sure on possible extra states (exotica) which can exist near the 'normal' ($q\bar{q}$) states. The second order problem concerns fitting different characteristics of the mesons such as the partial widths with more or less complex models in order to obtain more physical information on $q\bar{q}$ in the confinement region.

5. Acknowledgements

The author wishes to thank Prof. David Bugg for organizing this Summer School. He also wishes to thank his co-workers from the Obelix collaboration for helpful discussions.

6. References.

1. S. Godfrey and N. Isgur, Phys. Rev. D32 (1985) 189.
2. T.H.Bauer et al., Rev. Mod. Phys. 50 (1978) 261.
3. Y. Nambu, Phys. Rev. 106 (1957) 1366 ; W.R.Frazer and J.Fulco Phys. Rev. Lett. 2 (1959) 365, Phys. Rev. 117 (1959) 1603; J.J.Sakurai, Ann. Phys. 11 (1960) 1.
4. D. Schildknecht, Springer Tracts Mod. Phys. 63 (1972) 57.
5. J.J. Sakurai and D. Schildknecht, Phys. Lett. B40 (1972) 121; B41,489; B42,216; F.M.Renard, Proc. 7 th Renc. Moriond, ed. Tran Thanh Van.
6. C. Erkal and M.G. Olsson Z. Phys. C31 (1986) 615.
7. Particle Data Group, Phys. Rev. D50 (1994) 1173.
8. Particle Data Group, Rev. Mod. Phys. 56 No 2 part II (1984).
9. Particle Data Group, Phys. Lett. B170 (1986) 1.
10. A. Donnachie and A.B. Clegg, Z. Phys. C34 (1987) 257.
11. A. Donnachie and H. Mirzaie, Z. Phys. C33 (1987) 407.
12. F. Nichitiu, Models and Mathematical tools in meson spectroscopy. inv. talk, LEAP94 Sept 1994 Bled, Slovenia.
13. P wave resonant are in some phase-shift solutions in the analyses : A.D.Martin and M.R.Pennington, Ann. Phys. (NY) 114 (1978) 1 ; H.Becker et al., Nucl. Phys. B151 (1979) 46 ; M.J.Corden et al., Nucl. Phys. B157 (1979) 250 , and no P resonance in all four solutions of : B. Hyams et al., Nucl. Phys. B64 (1973) 134; B100 (1975) 205.
14. F.M.Renard, Basics of electron positron collisions,1981, Editions Frontiers, Gif sur Yvette, France.
15. D. Aston et al., Nucl. Phys. B189 (1981) 15.
16. M. Atkinson et al., Z.Phys. C26 (1985) 499.

17. M. Atkinson et al., Nucl. Phys. B231 (1984) 15; B243 (1984) 1; Z. Phys. C30 (1986) 531.
18. V.K. Henner and D.N. Wolfson, Conf. Hadron 93, Como, Italy, June 1993, Nuovo Cim. A107 (1994) 2511.
19. A. Donnachie and A.B. Clegg, Z. Phys. C42 (1989) 663.
20. D.Bisello et al., Phys. Lett. B220 (1989) 321.
21. M.E.Biagini et al., Nuovo Cim. A104 (1991) 363.
22. A.B.Clegg and A.Donnachie, Z.Phys. C45 (1990) 677.
23. J.M.Blatt and V.F. Weisskopf, Theoretical Nuclear Physics. New York, J. Wiley and Sons 1952, p.361; F.v. Hippel and C.Quigg, Phys. Rev. D5 (1972) 624.
24. D. Alde et al., Z. Phys. C54 (1992) 553.
25. D. Alde et al., Z. Phys. C66 (1995) 379.
26. A. Antonelli et al., Z. Phys. C56 (1992) 15.
27. M. Atkinson et al., Z.Phys. C27 (1985) 233.
28. Busenitz, Phys. Rev. D40 (1989) 1.
29. D. Bisello et al., Z. Phys. C39 (1988) 13.
30. D. Bisello et al., Z. Phys. C52 (1991) 227.
31. D. Aston et al., Nucl. Phys. B292 (1987) 693, B296 (1988) 493 ; P.F. Bird, Ph.D.-Thesis, SLAC Report 332 (1988).
32. D. Aston et al., SLAC-PUB-5721 (1991).
33. D. Aston et al., SLAC-PUB-5657 (1991).
34. L.P. Chen and W. Dunwoodie (mark III) SLAC-PUB-5674 (1991) , Int. Conf. Hadron 91,Univ. of Maryland at College Park, World Scientific 1992, pag.100.
35. S.I. Bityukov et al., Phys. Lett. B188 (1987) 383.
36. A.B. Clegg and A. Donnachie, Z. Phys. C40 (1988) 313.
37. A. Donnachie and A.B. Clegg, Z. Phys. C51 (1991) 689.
38. Yu.S. Kalashnikova, Workshop 'DAFNE', Frascati, April 1991, pag. 415.
39. A. Donnachie and Yu.S. Kalashnikova, Z. Phys. C59 (1993) 621.
40. F.E. Close and P.R.Page, preprint.Univ. of Oxford, OUTF-95-29P (1995).
41. D. Alde et al., Phys. Lett. B205 (1988) 397.
42. H. Aoyagi et al., Phys. Lett. B314 (1993) 246.
43. F. Nichitiu, Phase Shift Analysis in Physics of the Nuclear Interactions, Ed. Acad. Romania (Bucharest) (1980) ; Ed. Mir (Moskow) (Russian) 1983.
44. S.A. Sadovsky , preprint IHEP 91-75 (1991).
45. J.H.Lee et al., Phys. Lett. B323 (1994) 227.
46. C.Veneziano Nuovo Cim. 57 (1968) 190.
47. D.S. Peaslee, Conf. Hadron 89, Ajaccio,Corsica (France), sept. 1989, Editions Frontiers,Gif sur Yvette,p255.